energy&fuels

pubs.acs.org/EF

Review

Review on Improving the Performance of SiO_x Anodes for a Lithium-Ion Battery through Insertion of Heteroatoms: State of the Art and Outlook

Taeyeob Kim,[†] Hai Li,[†] Rafael Gervasone, Ji Man Kim,* and Jin Yong Lee*

Cite This: https://doi.org/10.1021/acs.energyfuels.3c00785

Read Online

ACCESS | Metrics & More | Article Recommendations

ABSTRACT: Anode materials for Li-ion batteries have attracted significant research interest owing to the growing demand for efficient and cost-effective energy storage systems. Among the various anode materials being studied, silicon-based anodes have garnered considerable attention as a result of their potential to overcome many of the limitations associated with graphite anodes. However, silicon-based anodes undergo high volumetric expansion during cycling, which results in anode failure. In contrast, silicon-oxide-based (SiO_x) materials exhibit limited volumetric expansion, making them viable candidates as anode materials in lithium-ion batteries. Despite this, there remain several challenges associated with SiO_x anodes, including volumetric expansion (160−200%), poor capacity retention, and low initial coulombic efficiency. To address these issues, the incorporation of heteroatoms into SiO_x anodes has been proposed as a promising strategy. In this review, we aim to provide an overview of the current state of research on SiO_x anodes, including experiments and theoretical calculations, with a focus on the insertion of heteroatoms to improve the anode performance. In particular, we examine the effects of heteroatom incorporation on the anode conductivity, lithium diffusion, durability, and initial coulombic efficiency. In addition, we present a design strategy for the insertion of heteroatoms into the SiO_x anodes. This review aims to provide a comprehensive understanding of the role of heteroatoms in SiO_x anodes and highlight the potential for further research in this area.

1. INTRODUCTION

Lithium-ion batteries (LIBs) are a type of secondary battery that can be repeatedly charged and discharged and have a high energy density and low self-discharge rate.[1−3] Currently, LIBs using graphite as an anode are one of the most widely used energy suppliers. In graphite-anode LIBs, Li ions are stored in the layered structure of graphite. Therefore, there is no significant change in volume, and the stability of the battery is increased.[4,5] In addition, the use of graphite is very economical because of its high coulombic efficiency (∼95%), decreased Li-ion loss, and low cost.[1,6,7] However, the low maximum capacity (372 mAh/g) of graphite is the main challenge faced by LIBs. In particular, as the demand for batteries with larger capacities for electric vehicles and energy storage has recently increased,[8−10] research on anode materials to replace low-capacity graphite has become more important. One of the most representative materials being studied is Si-based anodes. The theoretical capacity of the Si anode is approximately 4200 mAh/g, which is more than 10 times that of the graphite anode. However, because Si undergoes an alloying process, its volume expansion rate (up to 400%[11]) is considerably higher than that of graphite, resulting in limited cyclability. In addition, Li ions are continuously consumed during the lithiation/delithiation process because of the repeated formation of the solid electrolyte interface (SEI) layer, which leads to low coulombic efficiency. The low electron conductivity of Si also decreases the capacity of the battery.[12−14]

To overcome the limitations associated with silicon anodes, electrodes based on SiO_x have recently gained significant research interest (in the literature, SiO_x and SiO are often interchanged because an exact stoichiometry is typically not required or attained[15]). Although the atomic structure of SiO_x has been debated for nearly a century, it has been demonstrated to comprise a multiphase system, as shown in Figure 1A, where amorphous Si domains coexist with amorphous SiO_2, as assumed by the random mixture model, which is generally separated by an interphase boundary layer.[15,16] In SiO_x anodes, the lithium electrochemical process occurs via both Li−Si alloying and the reversible formation of lithium silicates, such as $Li_2Si_2O_5$, that participate in the

Received: March 9, 2023
Revised: May 20, 2023

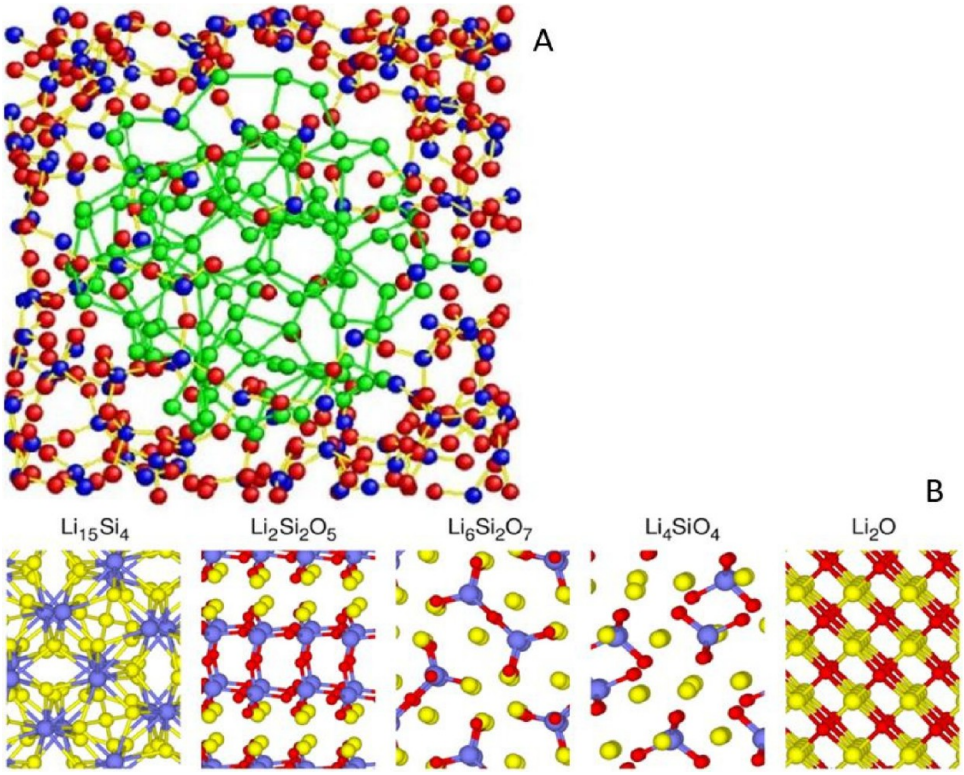

Figure 1. (A) Reconstructed model of the SiO heterostructure. Inner amorphous Si and the outer SiO_2 matrix are visible. This panel was reproduced with permission from ref 16. Copyright 2016 Springer Nature. (B) Simulated crystal structures of lithium oxides and silicates. The yellow, blue, and red balls represent lithium, silicon, and oxygen, respectively. This panel was reproduced with permission from ref 18. Copyright 2015 American Chemical Society.

lithiation/delithiation process.[17] Upon cycling, irreversible lithium oxides (Li_2O) and silicates (Li_4SiO_4 and $Li_6Si_2O_7$) (Figure 1B) are also formed. This translates into a reduced capacity and an increased cyclability compared to Si as a result of the ability of lithium composites to buffer volume expansion.[18] Lithiated silicon ($Li_{15}Si_4$) is less dense than lithium oxides and silicates. Hence, because the mass is concentrated in the latter materials, more volume is left free to accommodate $Li_{15}Si_4$ expansion.[15] It has been shown that a higher oxygen content of SiO_x corresponds to a lower capacity and better cyclability.[19] The initial theorical capacity of the SiO_x anode is 2615 mAh/g, and its volume expansion during lithiation/delithiation is ~160%[18] (typically between 100 and 300%[11]). One major limitation of the formation of Li silicates and oxides during the first cycle is the low initial coulombic efficiency (ICE), which must be addressed when relying on SiO_x-based anodes. ICE is commonly increased by pre-lithiation.[20,21]

The failure mechanism of the negative electrode of lithium batteries has been studied by many researchers,[22−24] and many corresponding solutions have been proposed on the basis of the electrode failure caused by different mechanisms.[25] The first is pulverization of the electrode. The phase transformation and volume issues faced by Li−Si alloys generated during the crystalline silicon and lithiation process generate considerable stress and cause pulverization of the electrode. As the Li ratio of the Li−Si alloy increases, the number of Si−Si pairs decreases and the volume of alloy increases up to about 300%.[26−28] Simultaneously, the large volume change causes the SEI layer to become unstable, which also wastes electrolytes, and forms an unreasonably thick SEI layer, causing the active material to be consumed.[29] On the basis of these factors, the battery structure will be slowly and irreversibly destroyed and become unusable. Therefore, the main root cause may still be the volume expansion problem and decrease in material activity. During the lithiation and delithiation of lithium batteries, the SiO_x-based anode is a buffer medium relative to pure Si, which can alleviate a certain degree of volume expansion. Although relevant techniques have made great progress in the past decade, lithium batteries with SiO_x as the anode material still cannot satisfy the growing demand for high energy and power density. Owing to these unavoidable defects, lithium batteries with SiO_x as the anode material cannot be widely used in industrial production. Current research efforts are expected to increase the pristine coulombic efficiency while extending the life of LIBs and maintaining high capacity. The reactions occurring on electrodes are the basis of electrochemical properties, and the morphology and microstructure have a significant impact on the electrochemical performance. Hence, the above three directions are basic ideas for solving the current problem of anode materials for SiO_x substrates. Therefore, measures to improve the performance of SiO_x-based anode materials include the following: (1) improved electrochemical performance through disproportionation reactions above 800 °C or with other ions,[30−32] (2) reducing the influence of the volume effect through material design and increasing the ICE value, and (3) improving the coulombic efficiency and cycle efficiency of the battery by doping, coating, modifying, binder design, electrolyte additives, and modifying the microstructure of SiO_x. Among the above methods, adding external heteroatoms can be a cost-efficient and simple approach, and

https://doi.org/10.1021/acs.energyfuels.3c00785
Energy Fuels XXXX, XXX, XXX−XXX

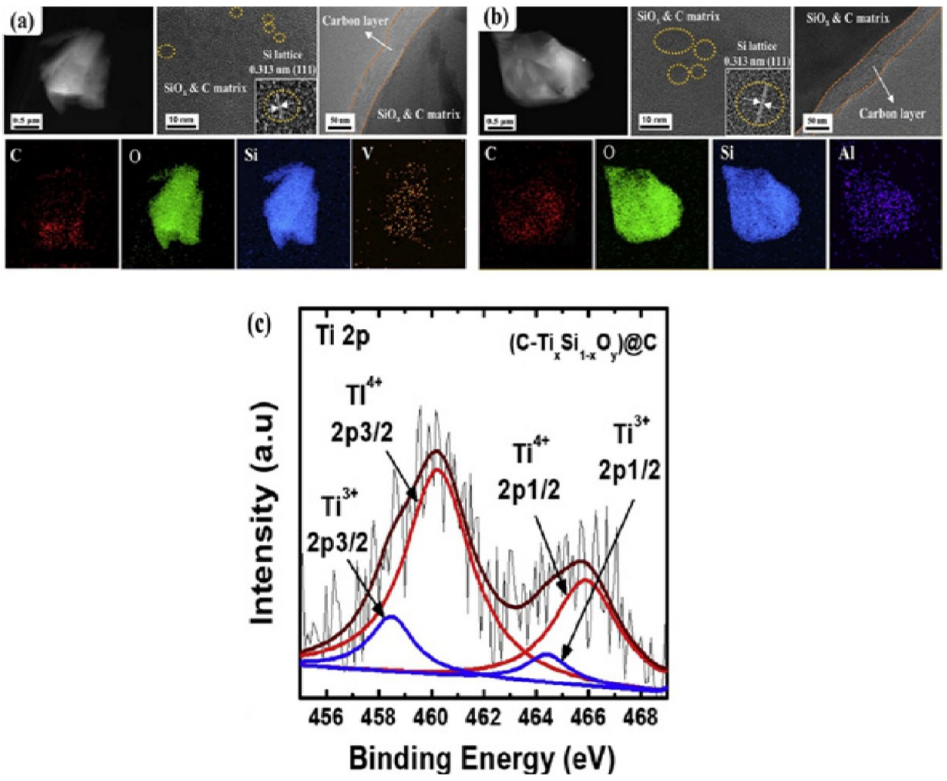

Figure 2. TEM and elemental mapping image of (a) V−SiO_x@C and (b) Al−SiO_x@C. This panel was reproduced with permission from ref 35. Copyright 2020 Elsevier. (c) Ti 2p XPS spectra of (C−$Ti_xSi_{1-x}O_y$)@C. This panel was reproduced with permission from ref 36. Copyright 2018 Elsevier.

there have been many excellent results, including both metallic and non-metallic SiO_x anodes. Current research is expected to focus on exploring materials that combine the advantages of both graphite and SiO_x materials.[33,34]

As aforementioned, SiO_x anodes have broad prospects for application in LIBs owing to their relatively low volume expansion and efficiency compared to graphite anodes. Currently, publications on SiO_x anodes increased by 40% from 2018 to 2022, and the frequency of citations has increased almost 4-fold. However, there exists a dearth of literature reviews on SiO_x composites comprising additional elements and differing structures, with consideration given to both experimental and theoretical calculations. This review highlights the improved properties and potential industrial and commercial applications of SiO_x in the presence of other heteroatoms or in combination with other materials. The purpose of this review is to offer support for those seeking to gain a comprehensive understanding of the current state of development in this field. Drawing on previous research, our aim is to provide a thorough overview that will serve as a resource for individuals seeking to expand their knowledge of SiO_x. Through our analysis, we hope to contribute to the ongoing discourse and provide a foundation for future research in this area.

2. SIO_X HETEROATOM ADDITION DESIGN

The incorporation of heteroatoms proved to be an efficient way to address many issues related to SiO_x anodes. From the selection of proper heteroatoms, doping can be exploited to increase the number of charge carriers and/or the conductivity of the anode material. In addition, many other interesting features of heteroatom doping of SiO_x may arise because of how the dopant induces modifications in the SiO_x lattice morphology. This could be exploited to increase the anode rate and cyclability. Doping not only improves the electrochemical performance by increasing the conductivity of the materials and adding charge carriers but also influences the material structure by facilitating an increased lithium diffusion rate or strengthening the material, thus enabling better cyclability. Dopant heteroatoms may also form inert species that can buffer volumetric changes, resulting in both increased cyclability and improved ICE. ICE can also be directly increased through the addition of lithium heteroatoms. The advantages of heteroatom doping of SiO_x anodes can be formally summarized as follows: improved electron conductivity, increased number of charge carriers, faster lithium diffusion rate, improved cyclability as a result of the stabilized structure, and higher ICE.

The first two effects are inherently typical of a doped system and mainly rely on how the dopant affects the electronic band structure of the material and the extra charge carriers as a result of p- or n-type doping. The last three effects are mainly due to modifications in the structure of the material following the insertion of the heteroatoms. These effects can be simultaneously exploited by tuning the doping system. In general, it is difficult to isolate just one such advantage when adding heteroatoms to an electrode; these properties are often found to be interdependent. Nevertheless, it is worth considering separately what factors make these types of improvements possible, taking some study cases as an example to better understand what ultimately determines the success of a doping system in each of these aspects.

2.1. Transition Metal Insertion and Structural Design.

2.1.1. Enhancing Electron Conductivity with Doping a

https://doi.org/10.1021/acs.energyfuels.3c00785
Energy Fuels XXXX, XXX, XXX−XXX

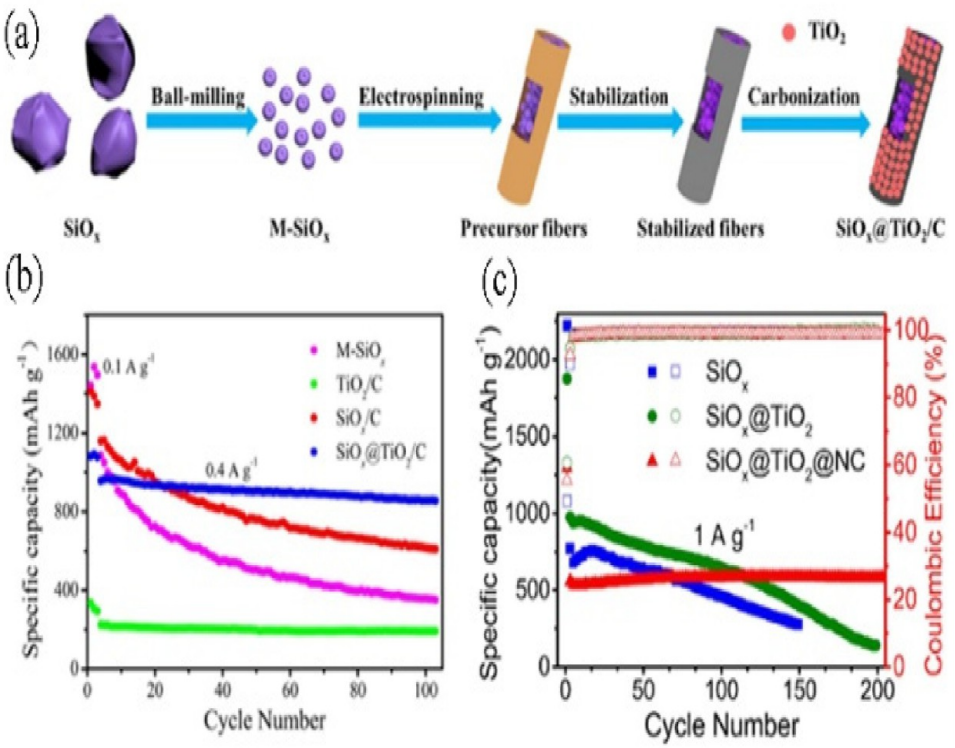

Figure 3. (a) Schematic of the preparation and (b) cycle performance of SiO_x@TiO_2/C. This panel was reproduced with permission from ref 38. Copyrght 2021 Elsevier. (c) Cycle performance of SiO_x@TiO_2/NC. This panel was reproduced with permission from ref 39. Copyrght 2022 Elsevier.

Transition Metal. Among the possible strategies for increasing the performance of SiO_x anodes, doping with transition metals has been widely explored, mainly to enhance the low electron conductivity of the SiO_x anode. Several attempts have been made to form p- or n-type doped composites by doping with metals. Doping an element with fewer or more valence electrons than Si is termed p- or n-type doping, respectively. In the former case, the positive holes formed in the valence band help electrons move. In n-type doping, more free electrons are generated, which increases electron conductivity. Kwon et al. fabricated V−SiO_x@C and Al−SiO_x@C complexes using an alcoholism method. X-ray photoelectron spectroscopy (XPS) confirmed the presence of V^{4+} and V^{5+} in V−SiO_x@C and Al^{3+} in Al−SiO_x@C. The V-doped composite underwent n-type doping with V^{4+}, and the Al-doped composite was formed by p-type doping with Al^{3+}. The elemental mapping images in panels a and b of Figure 2 also show that each metal was doped in SiO_x. Both of the doped composites showed higher performance than ordinary SiO_x@C composites, but V−SiO_x@C prevailed. The V-doped composite had a specific capacity of 1305 mAh/g at 0.1 A/g, and the Al-doped composite had a specific capacity of 1147 mAh/g, which was higher than that of SiO_x@C (911 mAh/g). In addition, after 600 cycles, the capacity of SiO_x@C was maintained at 86.7%, that of Al−SiO_x@C was maintained at 90.2%, and that of V−SiO_x@C was maintained at 93.0%.[35]

Yang et al. formed a n-type doped composite by doping Ti^{3+} with C-coated SiO_x using a solution-phase method. XPS data confirmed that Ti^{3+} and Ti^{4+} were mixed in the composite (Figure 2c); Ti^{3+} provides additional free electrons to the composite. In comparison to C−SiO_x or (C−SiO_x)@C, the n-type doped composite showed better performance. The composites coated with carbon exhibited initial discharge capacities of 390 and 851 mAh/g. In contrast, (C−$Ti_xSi_{1-x}O_y$)@C, the n-type doped composite had an initial capacity of 1304 mAh/g. In addition, the capacity retention of the doped composite also exhibited a value of 88.9%, which is higher than those of the other two reference anodes. Yang et al. also fabricated Ti-doped composites by increasing the concentration of Ti ions. In this case, as the amount of $TiCl_4$ added during composite formation increased, the specific capacity decreased. The composite containing 4.75 wt % Ti ions had a significantly lower specific capacity than that containing 0.21 wt % Ti ions. XPS results confirmed that the oxidation number of Ti in the 4.75 wt % Ti composite was almost 4+. This indicates that the degree of n-type doping can decrease as the amount of the used Ti source increases. In other words, simply using a larger Ti source is not helpful for increasing the electric performance; therefore, finding an appropriate ratio between the Ti source and other materials is important.[36]

Miyachi et al. synthesized three metal-doped SiO_x anodes using a co-evaporation process. The doped metals used were Fe, Ti, and Ni. The Ni-doped anode exhibited a high capacity retention of 82% after 400 cycles at the 1 C rate. In addition, the ICE of the metal-doped anodes was >84%, which is similar to that of graphite. Additionally, during the charge and discharge processes, the oxidation number of Si in the doped anodes changed from 0 to +4 with high reversibility. This resulted in a high coulombic efficiency of the metal-doped anodes.[37]

2.1.2. Transition Metal Oxide Coating for Stability. Meanwhile, some research has been conducted to stabilize the structure of SiO_x anode materials using metal oxides. The

https://doi.org/10.1021/acs.energyfuels.3c00785
Energy Fuels XXXX, XXX, XXX−XXX

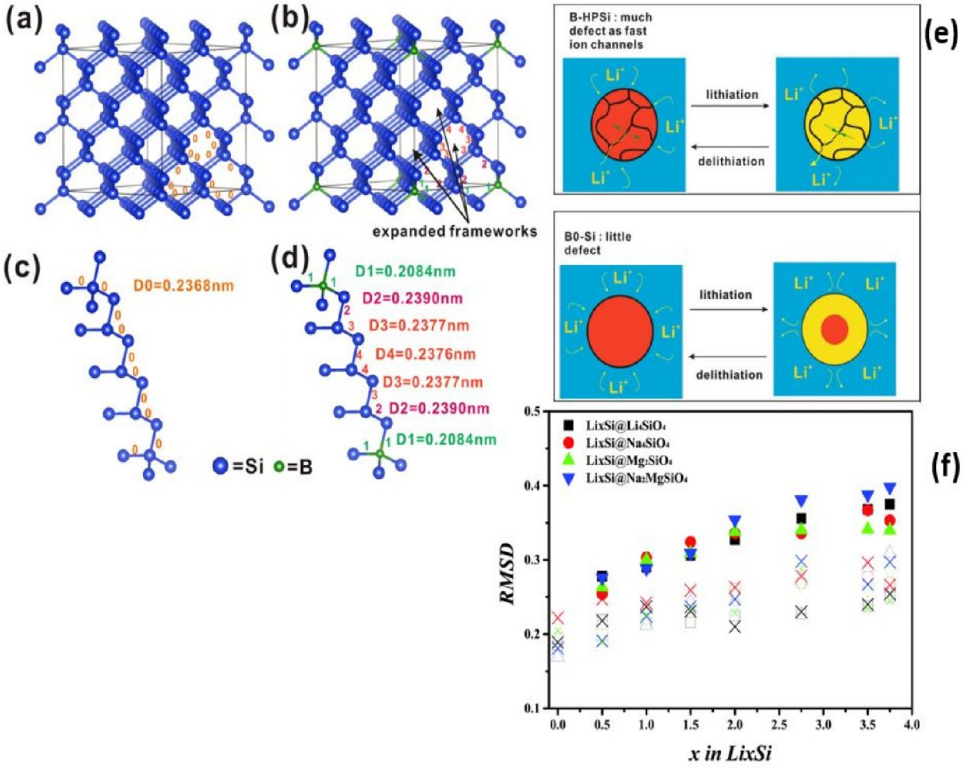

Figure 4. (a and b) Simulation of pure Si and B-doped Si. (c and d) Simulation of the nearest neighbor distance in pure Si and B-doped Si. (e) Schematic illustration of how local defects act as preferential pathways increasing lithium diffusion and homogeneity of lithiation. These panels were reproduced with permission from ref 45. Copyright 2019 American Chemical Society. (f) Root mean square displacement of lithium (solid shapes), silicon (hollow shapes), and oxygen (crossed shapes) as a function of x in Li_xSi for various alloys. This panel was reproduced with permission from ref 49. Copyright 2022 Royal Society of Chemistry.

metal oxide layer surrounding SiO_x alleviates the volume change during cycling.

Tan et al. synthesized the TiO_2 coating layer of the SiO_x@TiO_2/C composite derived from titanium isopropoxide (TTIP). As shown in Figure 3a, the TiO_2 layer serves as a physical buffer in this composite. This indicates that the TiO_2 layer can alleviate the volume change of SiO_x because of its smaller volume change than that of SiO_x. Therefore, cracks formed by the volume change during cycling decreased, followed by an increase in cycle retention. In comparison to the cycle retention of ball-milled SiO_x and carbon-coated SiO_x (32.3 and 52.5% after 100 cycles at 0.4 A/g, respectively), the capacity retention of the TiO_2/C-coated composite was considerably high (89.5%).[38]

Liu et al. used a TiO_2 coating layer to prevent side reactions during the synthesis of SiO_x@TiO_2/NC composites. The NC layer on SiO_x can act as a physical buffer that decreases the volume change of the anode. Liu et al. used a chitin solution as the source of the NC coating layer. Prohibiting the reaction between SiO_x and NaOH in a chitin solution was the main factor for the successful synthesis of the composite. Thus, a TiO_2 layer acting as a blocking layer was formed in advance. The TiO_2 layer successfully separated the two reagents and alleviated the volume change of the SiO_x-like NC coating layer. The SiO_x@TiO_2/NC composite exhibited a high discharge capacity of 633 mAh/g and a capacity retention of 92.3% at 0.5 A/g. However, SiO_x and SiO_x@TiO_2 exhibited lower capacity retention because of the high volume change of SiO_x.[39] It is noteworthy that TiO_2 has been successfully utilized in combination with graphite materials for incorporation into graphene-modified SiO_x anodes during the process of graphene exfoliation.[40] Given the extensive research and development of titanium dioxide, this material technology is highly mature and poised for further adoption in industrial settings.

2.2. Heteroatom-Insertion-Induced Changes in Li-Ion Diffusion Rates and Cyclability. This section presents a comprehensive summary of the impact of insertion with various metals and non-metallic elements, including carbon, on the apparent properties of anode materials. The successful implementation of silicon- and SiO_x-based anodes remains a significant challenge for achieving industrial application cycles. Previous research has indicated that the use of carbon-based materials is essential for improving the performance and stability of these anodes.[41] He et al.[42] have provided a comprehensive review of the progress made with silicon−graphite materials and have proposed several promising directions for their industrialization. One strategy that shows great potential is the utilization of three-dimensional (3D) cross-linked binders. As reported by Tang et al.,[43] these binders are capable of efficiently converting the strain energy of the anode material into other forms of energy through multiple hydrogen bond networks. Pre-lithiation is also effective in ensuring that Li^+ transport is not negatively impacted. In addition, studies on the SEI layer have highlighted the potential of double coating with amorphous carbon and $LiAlO_2$. This approach, as introduced by Yan et al.,[44] incorporates a traditional alumina coating into the modification of silicon-based and similar materials, which holds great promise for improving their performance and stability.

https://doi.org/10.1021/acs.energyfuels.3c00785
Energy Fuels XXXX, XXX, XXX−XXX

Table 1. Summary of Heteroatom-Inserted SiO_x Anode Batteries

anode	specific capacity (mAh/g)	current density	cycle number	capacity retention (%)	reference
V−SiO_x@C	1305 (anode)	0.1 A/g	600	93	35
(C−$Ti_xSi_{1-x}O_y$)@C	876 (anode)	1 A/g	600	88.9	7
SiO_x@TiO_2/C	855 (anode)	0.4 A/g	100	89.5	38
SiO_x@TiO_2@NC	633 (anode)	0.5 A/g	650	92.3	51
HB−SiO	947 (anode)	0.5 C	100	93.3	46
Mn-doped SiO nanoparticles	1600 (anode)	1 A/g	2000	almost constant	52
N−SiO_x@C	950.7 (anode)	4.2 A/g	100	91.4	48
N and P co-doped SiO−C@CNT	848 (anode)	0.1 A/g	1500	84	50
Li/B−SiO_x@C	1184.8 (anode)	0.5 C	250	85.4	53
Si@SiO_x/WCGC (1:2)	1125 (anode)	1 A/g	100	79.6	54

2.2.1. Faster Ion Diffusion Rate. The effect of heteroatom insertion on the lithium diffusion rate in SiO anodes can be understood in terms of the structural modifications induced by heteroatoms. The dopant-induced defects act as fast ion channels. This has been shown to be the case for the Si crystal structure, where boron insertion increases the Si−Si bonding distance (panels a−d of Figure 4), thus possibly reducing the energy barrier required for ion diffusion.[45] For example, in 2015, Woo et al.[46] achieved boron-doped SiO-based negative electrodes through a one-step spin-on dopant process. Although thermally treated SiO (H−SiO) exhibited improved electrochemical performance compared to non-treated SiO, they were able to further improve the electrochemical performance by doping H−SiO with boron. Disproportionation caused by heat treatment led to the formation of Si crystallites with sizes of 4 ± 1 nm in H-SiO with respect to SiO. Although there were no observable differences between H−SiO and HB−SiO visible by field emission transmission electron microscopy (FE-TEM) or X-ray powder diffraction (XRD) owing to the small amount of dopant, the effect of the existence of boron could be observed by Raman spectroscopy. A shift in the Si peak from 508 to 498 cm^{-1} was observed as a result of the distortion of the Si network by stresses caused by B doping. Doping not only provided a conductive path for electrons but also increased the lithium-ion diffusion coefficient from 9.28×10^{-12} to 4.25×10^{-11}. This allowed for a specific capacity of 947 mAh/g at 0.5 C with a capacity retention of approximately 93% after 100 cycles, without the need for a carbon coating.

Another heteroatom widely exploited in combination with silicon is phosphorus, which is the immediate subsequent element in the periodic table. Its application should therefore immediately be considered as a dopant in SiO_x anodes. Chen et al.[47] synthesized a phosphorus-doped Si/SiO_2/C anode material comprising doped Si coated with carbon and silica layers, which was prepared by ball-milling flake Si particles with polyvinyl butyral and phosphoric acid as additives. Elemental analysis showed a homogeneous distribution of Si, O, P, and C on the surfaces of the obtained particles. In addition to increasing the intrinsic conductivity and Li^+ diffusion rate, p doping suppresses the formation of Li_2CO_3 in the SEI film, resulting in a higher ICE. Doping also increases $Li_2Si_2O_5$ (active for lithiation/delithiation) while decreasing irreversible Li_ySiO_x. It is also worth considering that the phosphoric acid treatment increases the surface SiO_2 content by prohibiting the formation of less oxidized SiO_x. An ICE of 86.7% was achieved for the 7% doped electrode. It also showed an initial discharge capacity of 2860.3 mAh/g while retaining a capacity of 1389.8 mAh/g. Jin et al.[48] identified carbon-coated N-doped silica anodes as an environmentally friendly alternative to phosphorus doping. In fact, in addition to the increase in electron conductivity caused by the increased number of free electrons, N-doped silica also showed increased lithium-ion diffusivity. Indeed, similar to other heteroatom dopants, nitrogen causes the formation of shorter Si−N bonds, thus enlarging Si−Si bonds and improving lithium-ion migration. This resulted in an increased Li^+ diffusion coefficient of 8.78×10^{-15} cm^2 s^{-1} compared to 5.70×10^{-16} cm^2 s^{-1} for pristine SiO_x. Nitrogen doping also effectively reduced cracking upon cycling by suppressing volume expansion, resulting in a capacity retention of >90% after 100 cycles. The sole carbon coating enabled an expansion rate of 219%, while adding nitrogen dopant to the anodes limited the expansion rate to 156%. Nitrogen does not directly bind the expansion of the anode material because an increased lithium diffusion rate enables a more uniform volume expansion during lithiation/delithiation, thus reducing material fragmentation, resulting in a better performance.

This can be further understood by considering the work of Xie et al.,[49] who studied the lithiation behavior in four different doping systems, comparing Li−SiO to Na-, Mg-, and NaMg-doped SiO_x. They simulated the structures of these systems and their lithiation processes using *ab initio* molecular dynamics (AIMD). From a structural point of view, the Li−O distance in Li−Mg−SiO (as well as in Li−NaMg−SiO) was lower than that in Li−Na−SiO, which was interpreted as a sign of the better efficacy of Mg as a doping source with respect to Na, indicating a higher ICE. The volumetric expansions after lithiation were 97.63, 90.54, 118.78, and 86.43% for Li−SiO, Li−Na−SiO, Li−Mg−SiO, and Li−NaMg−SiO, respectively. The optimum result in the latter doping system can be attributed to the binary doping sources, leading to a more irregular and amorphous initial structure (i.e., a larger initial volume and, thus, a smaller relative volume expansion). From the observation of the root-mean-square deviation (RMSD) of Li in the aforementioned systems (Figure 4f), two stages can be distinguished on the basis of the Li concentration. At lower concentrations, the diffusion is slow and dominated by strong interactions between Si and O, resulting in inactive material formation and Li-ion loss. From a Li content of $x \approx 2$ in Li_xSi, Li diffusion is dominated by the Si−Li alloy formation. At this stage, the Li−NaMg−SiO system showed the highest RMSD for Li, indicating the optimum high rate capability. This additionally shows that multiple doping can help achieve a stable amorphous structure, leading to improved cyclability and rate capability. Siyu et al.[50] realized SiO_x−C composite materials co-doped with both nitrogen and phosphorus using a molecular polymerization method. SiO and carbon were

https://doi.org/10.1021/acs.energyfuels.3c00785
Energy Fuels XXXX, XXX, XXX−XXX

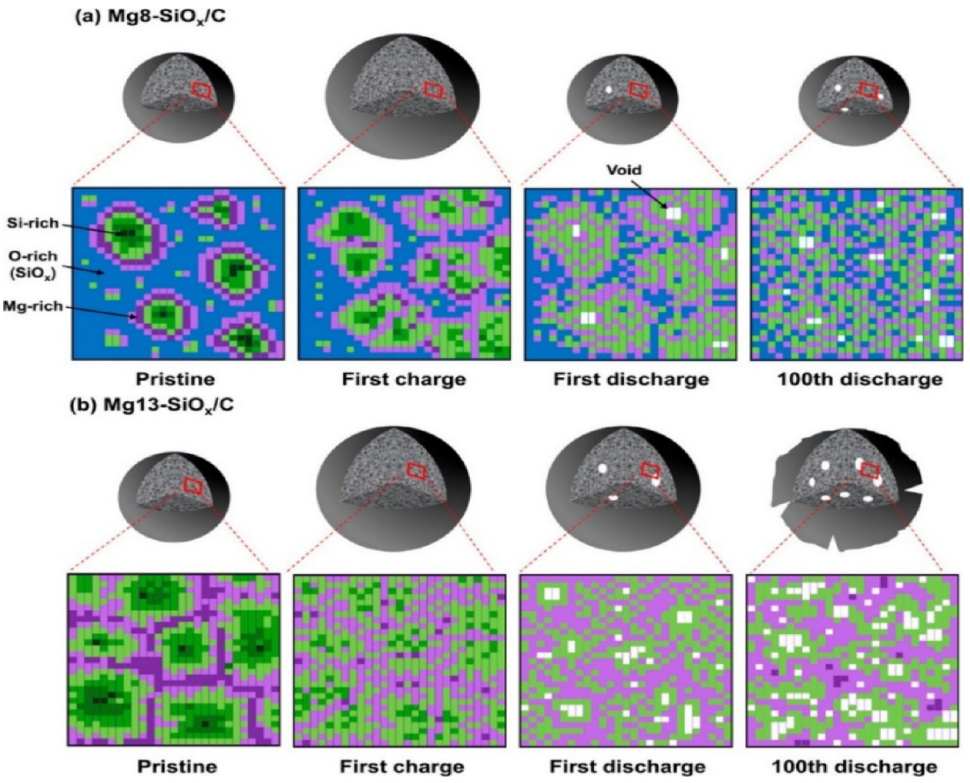

Figure 5. (a) Illustration of the cycling process reaction mechanism of Mg_8-SiO_x/C anodes. (b) Illustration of the cycling process reaction mechanism of $Mg_{13}-SiO_x/C$ anodes. This figure was reproduced with permission from ref 55. Copyright 2021 American Chemical Society.

uniformly dispersed at the atomic level along with the embedded carbon nanotubes. Three different colloidal solids were prepared and heated for 2 h in an argon atmosphere at 800, 900, and 1000 °C. The optimum electrode was the one treated at 900 °C, which consisted of irregular foam-like particles with a homogeneous distribution of Si, O, C, N, and P within the entire particle. Instead, the electrode treated at 800 °C showed many crystalline impurities, whereas the 1000 °C-treated electrode exhibited larger, denser, and partially crystallized SiO_2 particles, corresponding to less uniform materials. Doping, along with the embedded CNTs, favored rapid lithium-ion transport; this, in combination with the homogeneity of the SiO_x–carbon network, enables high capacity and cycling stability. In particular, the 900 °C-treated anode showed Li^+ diffusion coefficients ranging from 8.3×10^{-10} to 2.14×10^{-12} cm^2 s^{-1}. It also showed a reversible capacity of 848 mAh/g at 0.1 A/g and 84% capacity retention after 1500 cycles, while having an ICE of 54.5%. Some experimentally synthesized heteroatom-inserted anodes are listed in Table 1.

2.2.2. Homogeneity and Cyclability. As discussed in the previous paragraph, structural modifications as a result of heteroatoms often result in an increased lithium diffusion rate and improved stability. It is noteworthy to consider how the improved cyclability of the anode is often a consequence of a stronger binding network that can suppress volume expansion and the consequent anode failure. However, the results observed for nitrogen doping[48] suggest that an increased lithium-ion diffusion rate may have positive effects on the cyclability of the anode material, because this allows for a more uniform volume expansion. Therefore, homogeneity in volume expansion and structural homogeneity as well as a high lithium-ion diffusion rate are fundamental to improving the capacity retention in doped anode materials. For such improved cyclability to be effective, structural differences or multiple phases in the anode material should be avoided; otherwise, each part would show different volume expansion that leads to the localized cracking. Therefore, a proper dopant system design should consider the homogeneity of the anode material, which can be controlled by tuning the dopant concentration.

This was clearly demonstrated by Han et al.,[55] who compared three different levels of Mg heteroatoms, with Mg weight ratios of 0, 8, and 13%. As expected, a higher percentage of doping corresponded to a lower initial charge and discharge capacity and an increased ICE (increasing from 74.8% for the undoped specimen to 87.4% for the 13% Mg-doped specimen). However, the 8% doped anode showed the best retention, retaining >99% of its capacity, whereas the 13% doped anode had already decreased to 97%. Cross-sectional scanning electron microscopy (SEM) analysis showed that the volume expansion of Mg_8-SiO_x/C was minimal, with a swelling ratio of 22% after 100 cycles, whereas the swelling ratio was 72% for $Mg_{13}-SiO_x/C$. This is due to the recrystallization of Mg_2SiO_4, separating the material in Si- and Mg-rich domains, eventually causing phase separation. During subsequent cycling, the dissociation of the Mg- and Si-rich domains and their redistribution were observed. This implies a cycling-driven redistribution of dopants, leading to a relocation of the chemically inert phase. When Mg_8-SiO_x/C forms instead of $MgSiO_3$, crystallinity does not occur in any phase, supposedly as a result of the lower Young's modulus, which enables $MgSiO_3$ to conformationally fill the voids created by delithiated silicon. In addition, the mixing enthalpy of $MgSiO_3$ with Li silicates is lower than that of Mg_2SiO_4. This results in Mg- and Si-rich phases being more evenly distributed in the anode with 8% doping, suppressing void creation during

https://doi.org/10.1021/acs.energyfuels.3c00785
Energy Fuels XXXX, XXX, XXX−XXX

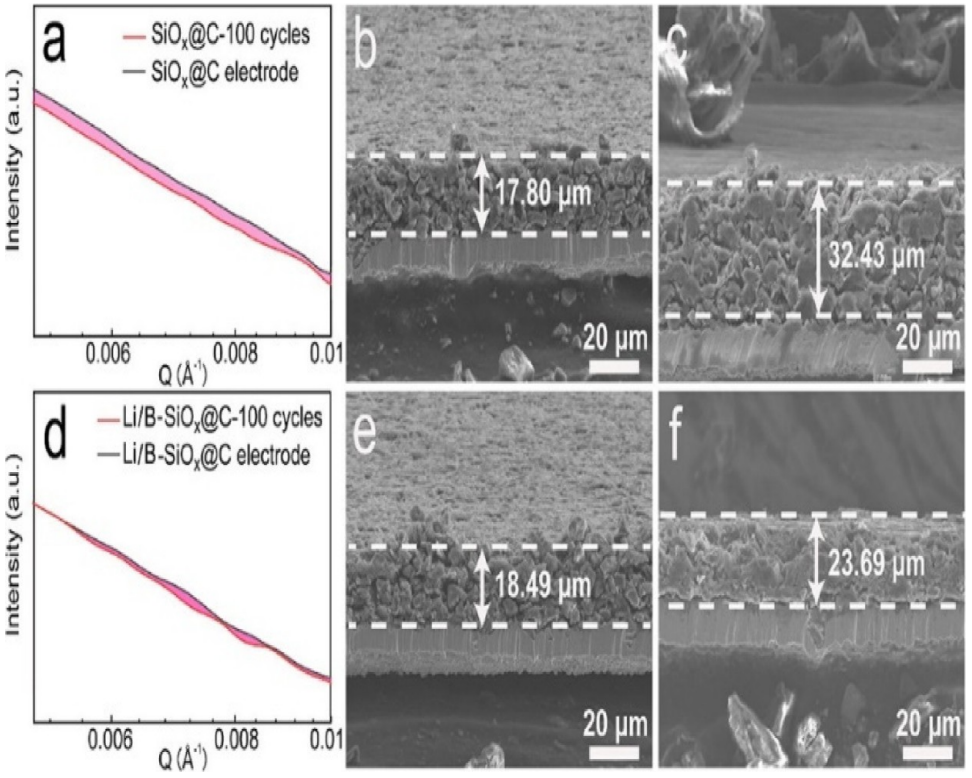

Figure 6. (a and d) Small-angle X-ray scattering before and after 100 cycles for an SiO_x@C electrode and a lithium−boron co-doped SiO_x@C electrode, respectively. (b and c) Cross-sectional SEM images before and after 100 cycles for the SiO_x@C electrode. (e and f) Cross-sectional SEM images before and after 100 cycles for the Li/B-SiO_x@C electrode. This figure was reproduced with permission from ref 62. Copyright 2022 American Chemical Society.

cycling, thus increasing the cyclability of the anode, as shown in Figure 5.

Tian et al. exploited the effect of the homogeneous distribution of magnesium silicates in Mg-doped SiO anodes.[56] They prepared micrometer-sized Mg-doped silica using a large-scale vacuum evaporation process. The bonding network of magnesium silicate effectively increased the structural strength of the micrometer-sized particles, enabling them to effectively withstand stresses during lithiation. After carbon coating, the as-prepared material exhibited a reversible capacity of >1400 mAh/g and 83% capacity retention after 200 cycles. It was also tested in 21 700 cells paired with $LiNi_{0.80}Co_{0.15}Al_{0.05}O_2$ as a cathode; it showed a capacity retention of >80% after 1000 cycles. $SiMg_yO_x$@C exhibited a much higher Li^+ diffusion coefficient after the first cycle (1.99×10^{-12} cm^2 s^{-1}) than undoped carbon-coated SiO (1.50×10^{-13} cm^2 s^{-1}). On the basis of the high-resolution transmission electron microscopy (HRTEM) images, nanodomains can be distinguished in SiO_x@C and lithium silicates, whereas only a pattern ascribed to $MgSiO_3$ could be observed in the Mg-doped anode. This demonstrates how the strong bonding network of magnesium silicate can effectively restrict the formation of Si and $Li_2Si_2O_5$ nanodomains, thus preventing the serious phase separation that occurs in SiO_x@C and induces pulverization of the microparticles. From the synergistic exploitation of the improved effects of heteroatom insertion on cyclability with the porous structure of an aerogel made of ultrasmall silica particles, Wang and Mao[52] realized a material with extraordinary capacity retention. From the doping of their materials with Mn heteroatoms, they were able to effectively enhance both electron transfer and Li^+ diffusion. This resulted in anodes with specific capacities of approximately 1800, 1600, and 1300 mAh/g at 0.5, 1, and 3 A/g, respectively. The specific capacitance was most significant after 2000 cycles at 5.0 A/g, resulting in an almost constant capacity of 1000 mAh/g.

2.3. Increasing ICE through the Addition of Heteroatoms and Efforts through Structural Design. An unavoidable problem with SiO_x is its low ICE. In general, in addition to the volume expansion problem, there are side reactions that influence ICE, resulting in cracking of the Si layer and formation of the thick SEI layer, which, in turn, leads to low ICE.[57,58] The formation of inert species upon the insertion of heteroatoms generally results in an increased ICE. The addition of heteroatoms, which can hinder the irreversible consumption of lithium ions during the first cycles, is the main way to avoid the low ICE usually associated with SiO. This can be done directly via pre-lithiation by directly adding lithium heteroatoms; however, lithium-free alternatives are also possible and often desired as a result of the lithium cost. With regard to the behavior of lithium heteroatoms added to a doped SiO_x system, Wan et al. showed that, when Li dopants are inserted into bulk silicon at concentrations below $x = 0.125$, Li atoms tend to separate from each other, resulting in a homogeneous dopant distribution. Instead, when Li dopants are inserted in bulk crystalline silicon at intermediate doping levels ($x = 0.125$), a local distortion of the host lattice with frequent breaking and reforming of Si−Si bonds is induced, whereas higher doping levels ($x \geq 0.1875$) cause a disruption of the host lattice, permanently breaking the Si−Si bonds. This induces negatively charged zones, ionizing nearby Li impurities and attracting them.[59] Lithium doping can be exploited as an alternative method of pre-lithiation to increase the ICE of SiO_x

https://doi.org/10.1021/acs.energyfuels.3c00785
Energy Fuels XXXX, XXX, XXX−XXX

anodes, thus addressing one of the main fundamental issues related to this type of anode material. Exploiting a suitable dopant facilitates its use as a volume buffer and avoids the need for active Li-ion consumption to form Li_2O or Li_4SiO_4 during the initial cycle.

In 2005, Tabuchi et al.[60] used a chemical synthesis process to obtain Li-doped SiO anodes. The resulting anode was able to overcome the irreversible reactions caused by the consumption of Li sources. Therefore, this may be a way of increasing the anode ICE while avoiding other expensive pre-lithiation methods, such as stabilized lithium metal powder (SLMP). The possibility of using lithium doping as an alternative to other pre-lithiation techniques was also clearly shown by Reynier et al.[61] by studying the implementation of carbon-coated Li-doped SiO_x anodes in 21 700 cells. The first-cycle efficiency is clearly improved by lithium doping because some of the irreversible silicates were already formed. From the increase of the amount of dopant, the SiO_2 nuclear magnetic resonance (NMR) peak became smaller until it vanished, whereas peaks of $Li_2Si_2O_5$ and Li_2SiO_3 were formed. At higher doping levels, only Li_2SiO_3 was formed, resulting in an ICE of 90%.

Steric considerations show that the reasonable upper limit of the SiO ratio in a 2700 cell design is approximately 40%. Considering heteroatoms apart from lithium, only Mg happens to be currently used in commercial applications for improving the ICE; in their work, Xie et al.[49] used AIMD to compare the effect of different doping systems on the lithiation behavior of SiO anodes. They concluded that a combined Na−Mg multi-dopant system can efficiently reduce the loss of active lithium, resulting in an increased ICE and reduced volume expansion. Li et al. reported a co-doped SiO_x electrode (in the form of carbon-coated-doped SiO_x)[66,62] via lithium/boron co-doping. Lithium is expected to reduce Li-ion losses during the first cycle, thus increasing the ICE. Boron is expected to increase Li-ion diffusion and strengthen the internal bonding enhancement rate and cycling stability. On the basis of inductively coupled plasma optical emission spectrometry (ICP−OES) characterization, the reported content of the Li dopant was 3.12%, whereas the content of B was 1.45%. As expected, Li doping increased the ICE by 83.3% compared to 78.9% for non-doped SiO_x@C. Lithium/boron co-doping effectively hindered the volume expansion (Figure 6), thus suppressing cracking and pulverization, which significantly increases the cycling and rate performance, allowing for an 85.4% capacity retention after 200 cycles. For the Li/$BSiO_x$@C and graphite composites, both an ICE and capacity retention of >90% can be achieved after 250 cycles. Once a stable coulombic efficiency (>95%) of graphite electrodes can be achieved, the large-scale commercial application of SiO_x will ensue.

To solve the volume expansion problem of SiO_x anodes, there are generally two widely explored approaches: (1) reducing the size of SiO_x[63] and (2) introducing heteroatom metals and carbon.[64−67] In addition, some biomass is also added to the anode. Although its lithium storage function is not very good, it plays a role in limiting the expansion of SiO_x.[54,68,69] The first approach uses the internal void space to allow silicon and SiO_x nanostructures to expand and contract without disrupting the connection between particles. The second approach uses heteroatoms to achieve better conductivity than SiO_x and to establish a stronger skeleton structure. These two methods can be used simultaneously in practical applications. In 2012, Choi et al. studied the decay mechanism of a composite Si/SiO_x/C anode under carbon coating.[70] During the characterizations using XRD, transmission electron microscopy (TEM), scanning transmission electron microscopy (STEM), and SEM, the first 10 cycles were used as the activation steps. Coulombic efficiency increased. Subsequently, local and global attenuation gradually occurred. In the two-dimensional (2D) structure design, Qi et al. performed electrochemical performance characterization on the anode of the core−shell structure under different thicknesses (0.8−9.7 nm) and determined that only 2−3 carbon layers (0.8−1.0 nm) can be greatly improved. Thicker carbon layers are not conducive to improved anode performance. In the 3D structure, there are currently several relatively mature structural designs, namely, core−shell,[71−73] yolk shell,[74,75] porous shell,[69,76,77] and honeycomb,[78] and some combined with other 2D structures.[79] These structures are relatively stable and exhibit excellent performance. Therefore, the pomegranate structure[80,81] has become widespread in recent years. Nanostructures can reduce the fragmentation caused by volume expansion; however, the large exposed surface of the nanostructures leads to side reactions and reduces the coulombic efficiency. The pomegranate structure exhibits advantages in that the nanoscale primary particle size prevents cracking and the internal void space allows for silicon expansion. The carbon skeleton functions as the mechanical backbone and electron conduction path, limiting the additional generation of SEI layers. After synthesis for the first time in 2014, research on this structure has been on the ascent,[82] and it has also performed well in lithium−sulfur batteries.[83]

2.4. Modeling Structure and the Simulation Process.

With the development of multiple high-resolution characterization techniques, the SiO_x model is becoming increasingly realistic.[16,84] However, owing to the true thermodynamic instability of SiO_x, the real microstructure of SiO_x in applications may be more complicated.[85] It is necessary to study the real structure of SiO_x and the changes in the macroscopic properties of anode materials that can be caused by changes in the microstructure. First-principles calculations based on the density functional theory (DFT) have been widely used to calculate and predict material properties. Through DFT calculations and AIMD methods, which are currently being used more widely, it is possible to obtain reasonable anode material candidates before finding suitable synthesis methods. At the same time, some studies have proven that the material can be effectively calculated using reactive molecular dynamics, in terms of dynamic simulation, and new force fields have been discovered one after another and have been a good fit to the properties of SiO.

There has been research on the lithiation of silicon dioxide itself for a decade. Yamamura et al.[86] calculated the formation energy of Li insertion at vacant sites within crystalline SiO_2 and amorphous SiO_2 and the formation energy of Li on the ring structure. On the basis of these calculations, the study established that amorphous silicon oxide possesses a substantial capacity for lithium storage and that lithium interacts with distorted SiO_4 tetrahedrons. These findings were confirmed in subsequent studies. After 3 years, research was conducted on the surface mechanism of silicon dioxide thin films. Lithium ions bind to silica by breaking the internal Si−O and Si−Si bonds within the silica and forming a lithium silicate structure. During lithiation, the partial reduction reaction leads to the formation of Li-containing defects and lowers the bandgap, and the conversion to Li_2O and Li_4SiO_4 at

https://doi.org/10.1021/acs.energyfuels.3c00785
Energy Fuels XXXX, XXX, XXX−XXX

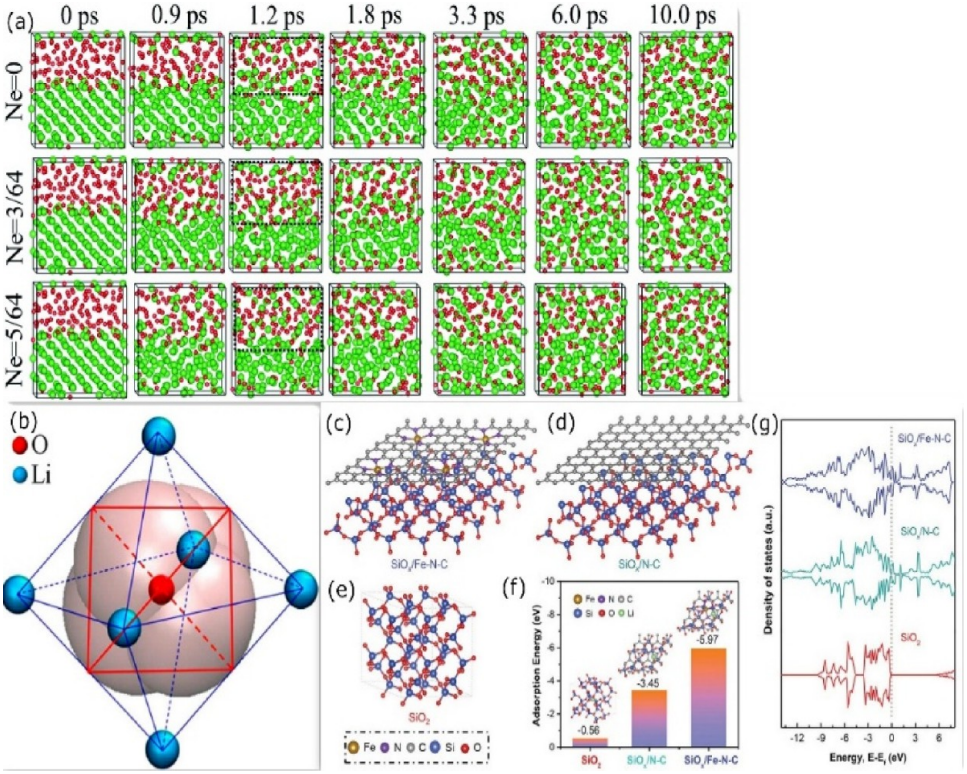

Figure 7. (a) Structure snapshots of Li and Si with different extra electrons (Ne) at different simulation times. This panel was reproduced with permission from ref 87. Copyright 2014 Royal Society of Chemistry. (b) Isosurfaces of the maximally localized Wannier function for the occupied 2s and 2p states of O^{2-} in the $[Li_6O]^{4+}$ complex. This panel was reproduced with permission from ref 88. Copyright 2013 American Chemical Society. (c–e) Diagrams showing the different structures of SiO_2/Fe–N–C, SiO_2/N–C, and SiO_2. (f) Lithium adsorption energies. (g) DOS calculation result. These panels were reproduced with permission from ref 51. Copyright 2022 John Wiley and Sons.

the interface is irreversible. This leads to an increased lithium storage. Other studies on silicon oxide films have shown that more efficient silicon dioxide anodes can be obtained by adjusting surface functional groups. During lithiation, the intercalation of lithium ions into the semiconductor leads to amorphization of the anode semiconductor material. Wang et al.[87] proved that the electron-rich effect is an important reactive factor in the amorphization process. It was also demonstrated that, in an electron-rich environment, the energy barrier decreases and diffusivity increases. The reduction in the diffusion barrier is due to the relaxation of the Si–Si bond with extra electrons. The study by Wang et al. highlights that lowering the energy barrier by 0.2 eV can change the Li mobility by a factor of 3000 at room temperature, as another strong proof that the Li–Si boundary is affected by electron-rich effects. Figure 7a shows that, at 1.2 ps, owing to the difference in electron concentrations, the diffusion of Li and Si was different, whereas at 10 ps, the two were almost completely mixed. The mechanism is not the formation of new holes but the accumulation of more electrons at the interface as a result of the electron-rich effect, thus resulting in a more thorough lithiation of Si.

2.4.1. Lithiation and Electrochemical Properties. SiO_x, which has an indeterminate stoichiometry number, is often heterogeneously composed of amorphous silicon and silicon dioxide. In the previous section, we described the simulation of the lithiation process. Most of the calculations are performed using software, such as Vienna *Ab initio* Simulation Package (VASP), for structural calculations and then for AIMD calculations.

Chou and Hwang[88] constructed a reasonable a-$Li_xSiO_{1/3}$ alloy model and studied the structural evolution and bonding mechanism of silicon-rich oxides using the AIMD method. The study by Chou and Hwang proved that silicon-rich materials with a low oxygen content can promote lithiation, but the ratio of oxygen to silicon is limited; otherwise, Li_2O is generated, leading to capacity loss. The electronic structure was investigated by analyzing the Bader charges, and the analysis proved that the fully lithiated coordination state of Li and O at the microscopic level was a 6-fold coordination octahedral $[Li_6O]^{4+}$ with Oh symmetry (Figure 7b).

Jung et al.[18] calculated the formation energies of Li, Si, and SiO under different ratios to obtain the most thermodynamically stable Li_xSiO with a corresponding theoretical specific capacity of 3172 mAh g^{-1} (x = 5.22). They also determined that the smaller volume expansion of SiO_x materials than that of silicon-based materials can be explained from the perspective of the atomic volume on a microscopic level, and the role of oxygen constrains the surrounding lithium atoms. Subsequently, new simulations of the lithiation process appeared one after another. Sivonxay et al.[89] investigated the amorphous structure and structural evolution of Si and SiO_2 and the lithium lithiation process from a thermodynamic perspective. It was found that the SiO_2 surface can generate Li_2O during cycling and hinder Li transport under conditions of low Li content, which seems to indicate a valuable direction for the surface design of materials.

Some studies have demonstrated that multiple doping systems are more efficient than single doping systems. Xie et al.[49] compared the effects of different doping systems on the

https://doi.org/10.1021/acs.energyfuels.3c00785
Energy Fuels XXXX, XXX, XXX−XXX

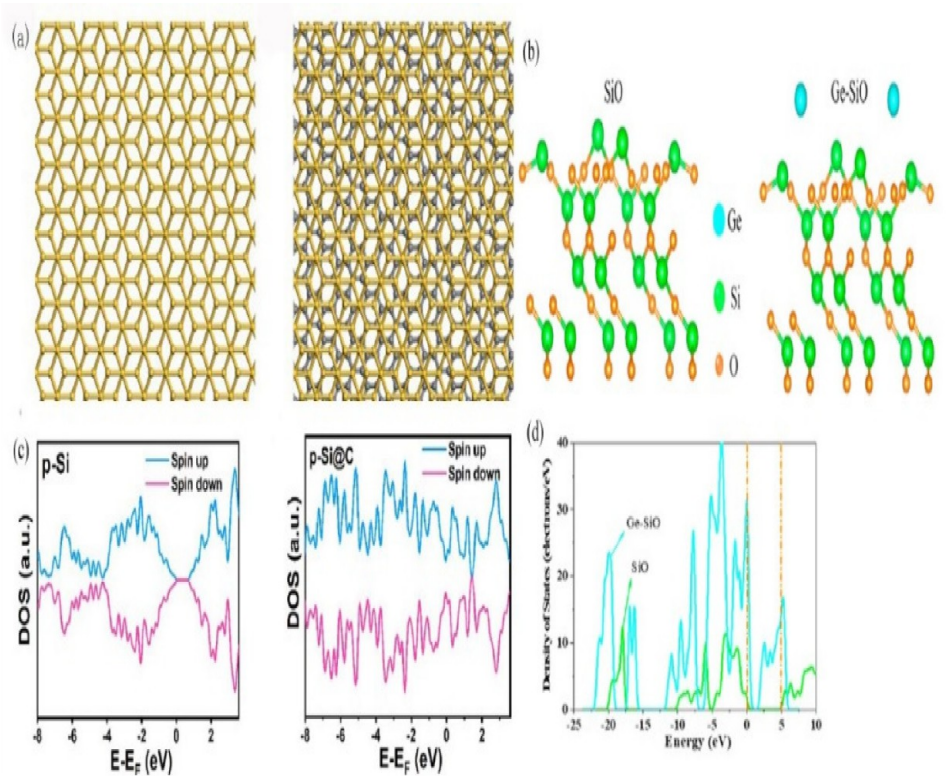

Figure 8. (a) Model of p-Si and p-Si@C. (b) Optimized SiO configuration and Ge-adsorbed SiO configuration. (c) DOS of porous Si and p-Si@C. These panels were reproduced with permission from ref 90, Copyright 2022 Elsevier. (d) Total DOS of the structure in panel b. This panel was reproduced with permission from ref 92. Copyright 2022 Elsevier Ltd. and Techna Group S.r.l.

lithiation behavior of SiO anodes via AIMD; they concluded that a combined Na−Mg multi-dopant system can efficiently reduce the loss of active lithium, resulting in an increased ICE while also reducing the volume expansion. In their study, they investigated four different metal-doped SiO_x systems, Li−SiO, Na−SiO, Mg−SiO, and NaMg−SiO, and calculated their structures. The evolution, voltage distribution, and energy properties demonstrated their physical and electrochemical properties. The electronic structure changes during lithiation can be obtained by calculating the density of states (DOS), and different systems show similar DOS patterns, albeit with some minor differences. Presumably, this difference was due to the few Martian atoms in the amorphous structure. Previous studies have demonstrated that doping with transition metals maintains an amorphous state, which can affect the cell performance. In the DOS diagram, the energy-band center of Si changes dynamically during lithiation. Owing to the multi-doping in this study, the structural changes in the battery reaction are more complicated. The more obvious conclusion is that stable Si−Mg bonds lead to lower energy-band centers and Si−Li bonds lead to higher energy-band centers. In other words, the incorporation of metal accelerates the speed of change of the anode material to the conductor state during lithiation. In another study,[51] the DOS diagram of SiO_x dispersed in a nitrogen-doped carbon framework also revealed some properties, such as electrical conductivity (Figure 7g). On the basis of the calculations of the DOS and adsorption energies, the effect of the Fe single atom was mainly related to the Fermi level difference; this calculation result was also in good agreement with the experimental results.

Liu et al. synthesized a carbon-coated porous silicon material (p-Si@C) through magnesium thermal reduction.[90] The results of the DFT calculations were consistent with their expectations. Figure 8a provides a graphical representation of p-Si and the effect of the addition of a carbon layer. The DOS diagram in Figure 8c reveals that the bandgap of uncoated p-Si is 1.40 eV. However, the addition of a carbon layer dramatically enhances the conductivity of the material by narrowing the bandgap. The research conducted by Zhu et al.[91] aimed to investigate the influence of germanium (Ge) on Li diffusion. Although the study did not explicitly consider SiO_x, the findings are still applicable to SiO_x, owing to the formation of silicon during the disproportionation reaction. With different ratios of Ge, isovalent isomorphism can produce two types of results owing to the local expansion effect and the narrow-channel effect. With the increase of the Ge content, the narrow-channel effect gradually suppressed the local expansion effect. After the combination of the experiments and theoretical simulations, they determined that the most appropriate Si/Ge ratio was 15:1. This type of anode can decrease Li trapping by 70% and achieve and ICE of 94.1%, which is difficult to accomplish. Subsequently, Yu et al.[51] studied the improvement in anode performance by coating Ge on the surface of SiO based on the research of Zhang et al.[92] From the construction of a model of Ge adsorption on the SiO surface (Figure 8), the DOS and bandgap diagrams of the different states were calculated. As a result, the introduction of Ge led to a decrease in the bandgap from 4.924 to 0.011 eV, an increase in the quantum states near the Fermi level, and an increase in the conductivity of the anode. The effect of Ge on improving the overall electronic conductivity was similar to that of the other heteroatoms mentioned above. The only questionable point was that they adopted the ultrasoft pseudopotential method, and the projector-augmented wave

https://doi.org/10.1021/acs.energyfuels.3c00785
Energy Fuels XXXX, XXX, XXX−XXX

method described this system better unless the accuracy requirements are not too high.

2.4.2. Advances in Molecular Dynamics (MD) Simulation and Other Simulation Methods. The reactive force field[93,94] (ReaxFF) is a widely utilized MD force field that has been developed over many years to study the chemical reaction[95] of hydrocarbon and LIB electrodes.[96,97] Jung et al.[98] developed new parameters for Li and Si by first principles and applied them to ReaxFF. In terms of volume expansion, nanowires (NWs) with a SiO_x structure can have a lower volume expansion while having a higher Li concentration. Their results indicate that the volume change problem of SiO_x materials with thin layers of silicon dioxide is not obvious, possibly because of the suppression of volume expansion by stress. Li insertion into crystalline Si was studied in 2015. According to Ostadhossein et al.,[99] the lithiation process is accompanied by stripping of the c-Si layer, which occurs when the local lithium concentration is too high, thus indirectly proving the necessity of a buffer layer, such as amorphous SiO_x. The study conducted by Ge et al.[100] on the binuclear TiO_2/SiO_x@C material following the magnesia thermal reaction is of significant interest. Their findings indicate that capacitive behavior plays a crucial role in the pseudocapacitance of the material and suggest that slight cracking within the material can enhance its storage capacity by producing defective phase interfaces. These results underscore the importance of AIMD simulations in furthering our understanding of the behavior of advanced materials. Currently, there are also some physical field simulation methods[101] used in the simulation of lithium batteries; however, they are mainly used to simulate positive electrode materials, and there are limited articles on negative electrode materials.

Despite the considerable progress made in simulating the SEI layer[102] and the electrochemical decomposition of electrolytes[103] on anode surfaces as well as the formation of lithium dendrites,[104] LIB research must continue to highlight the investigation and enhancement of silicon-based anodes and SiO_x-related materials. One particularly promising avenue for the development of future LIB anodes is the incorporation of heteroatoms into the SiO_x materials. This strategy has the potential to result in a higher ICE and mitigate the volume changes associated with Li cycling.

3. CHALLENGES AND PERSPECTIVES

Although promising, the main challenge now involves finding a way to overcome the many limitations that still hinder large-scale applications, for which different approaches are currently being studied. The proper design of the heteroatom insertion system, meaning its choice, ratio, and spatial distribution, proved to be fundamental to properly tune the anodic material properties, attaining one or more advantages. The selection of a dopant capable of properly modifying the electronic bands of the material and/or performing n- or p-type doping can be exploited for better electronic properties. Thus, future research in this area should be directed toward exploring the distinctive properties associated with various 3D structures, such as hollow structures and pomegranate-like structures. Structural modifications as a result of dopant insertion can help increase lithium diffusivity, thus attaining more homogeneous lithiation across the material, resulting in an overall reduced volume expansion as well as the formation of inert species able to buffer volume expansion and the formation of a stronger binding network, which can significantly improve the cyclability of SiO_x anodes. Furthermore, the formation of inert species with inserted heteroatoms can prevent the irreversible consumption of active Li, which is the main reason for the poor ICE exhibited by SiO_x. It is worth considering how fundamental research on this topic is still fragmented, and no systematic investigation of many phenomena governing these systems is available; therefore, future research is expected to address heteroatom insertion effects at a more fundamental level, particularly by exploiting molecular simulations, thus providing a rationale for designing heteroatom insertion. This would allow for an easier design of more complex heteroatom-incorporated anodes, exploiting the features of a multi-component-doped system, in which two or more different types of heteroatoms act synergistically to achieve highly efficient anodes. In the field of simulation, the predominant focus of dynamic simulations is on pure SiO or pure silicon systems. However, DFT calculations are typically confined to small doped systems and are unable to provide insight into the dynamic performance of electrodes. As such, it is recommended to integrate the advantages of both approaches by utilizing DFT calculations to analyze the properties of composite material SiO_x. This can be achieved through methods such as cell expansion or by introducing lithium ions to assess changes in the structure of the system during the process of lithiation. This integrated approach can potentially lead to a more comprehensive understanding of the dynamic behavior of electrodes. As an example, a comparison of graphite and MXene coatings of the same thickness can be used to assess the efficacy of each modification method in terms of the conductivity and deformation of SiO_x negative electrodes. This analysis can help to identify the strengths and weaknesses of each approach.

4. CONCLUSION

SiO_x is a valid anode material candidate for lithium batteries, attracting growing interest in recent years. SiO_x anodes have the potential to be improved through the insertion of heteroatoms. In this brief review, from an analysis of the present scientific literature, we showed how the incorporation of heteroatoms into a SiO_x anode can be helpful in addressing most problems related to this type of anode. Furthermore, the development of realistic models of SiO_x and the need to study the real microstructure of SiO_x to understand the changes in macroscopic properties were mentioned. We briefly summarize the lithiation process and progress of some computational simulations. Some reasonable DFT and MD calculations are of great significance for the design of materials. Owing to the different element ratios in SiO_x, it is more important to explore the microscopic mechanism of Si, O, Li, and doping elements in the battery reaction process, and the simulation also saves the cost of trial and error. Overall, SiO_x shows promise as a great potential anode material for LIBs.

AUTHOR INFORMATION

Corresponding Authors

Ji Man Kim − *Department of Chemistry, Sungkyunkwan University, Suwon 16419, Republic of Korea;* orcid.org/0000-0003-0860-4880; Email: jimankim@skku.edu

Jin Yong Lee − *Department of Chemistry, Sungkyunkwan University, Suwon 16419, Republic of Korea;* orcid.org/0000-0003-0360-5059; Email: jinylee@skku.edu

https://doi.org/10.1021/acs.energyfuels.3c00785
Energy Fuels XXXX, XXX, XXX−XXX

Authors

Taeyeob Kim − *Department of Chemistry, Sungkyunkwan University, Suwon 16419, Republic of Korea*

Hai Li − *Department of Chemistry, Sungkyunkwan University, Suwon 16419, Republic of Korea*

Rafael Gervasone − *Department of Chemistry, Sungkyunkwan University, Suwon 16419, Republic of Korea; Department of Chemistry, Materials Science and Chemical Engineering (CMIC), Politecnico di Milano, 20133 Milano, Italy*

Complete contact information is available at: https://pubs.acs.org/10.1021/acs.energyfuels.3c00785

Author Contributions

†Taeyeob Kim and Hai Li contributed equally to this work.

Author Contributions

Taeyeob Kim, conceptualization, investigation, formal analysis, and writing—original draft; Hai Li, conceptualization, investigation, formal analysis, writing—original draft; Rafael Gervasone, investigation, formal analysis, and writing—original draft; Ji Man Kim, project administration, conceptualization, writing—review and editing, and supervision; and Jin Yong Lee, project administration, conceptualization, writing—review and editing, supervision, and funding acquisition.

Funding

This work was supported by the National Research Foundation (NRF) grant funded by the Korean government (2019R1A6A1A10073079 and 2022R1A4A1032832). JYL acknowledges the support by SKKU Global Research Platform Research Fund, Sungkyunkwan University, 2022.

Notes

The authors declare no competing financial interest.

Biographies

Taeyeob Kim received a bachelor's degree in chemistry from Sungkyunkwan University, Korea, in 2022. He is currently doing a master's course at Sungkyunkwan University under the supervision of Prof. Ji Man Kim starting from the spring of 2022. His scientific interests include synthesizing mesoporous silica materials and the anode materials composed of Si and carbon for a LIB.

Hai Li received a bachelor's degree in chemistry from the School of Chemistry and Chemical Engineering, Shanxi University. He is currently pursuing a combined master's and doctoral degree at Sungkyunkwan University under the supervision of Prof. Jin Yong Lee starting from the spring of 2022. His research interest includes the DFT calculation of nanomaterials and AIMD calculation of catalysts.

Rafael Gervasone received his bachelor's degree in materials engineering and nanotechnology in 2021 at Politecnico di Milano, where he is currently pursuing a M.Sc. degree in the same field, with a major focus on surfaces, interfaces, and colloids.

Ji Man Kim received a Ph.D. degree in chemistry at 1999 from the Korea Advanced Institute of Science and Technology (KAIST) and performed his postdoctoral research at the University of California, Santa Barbara for 2 years. Prior to joining the Department of Chemistry at Sungkyunkwan University as a professor at 2005, he was a senior researcher at the Korea Research Institute of Chemical Technology (KRICT) and an assistant professor at Ajou University. His research is focused on the design and synthesis of various nanostructured materials and their applications in energy and environmental fields.

Jin Yong Lee graduated and obtained a Ph.D. degree (chemistry) from Pohang University of Science and Technology (POSTECH), supervised by Prof. Kwang S. Kim, in 1997. He worked with Prof. David Chandler at the University of California, Berkeley as a postdoc and with Prof. Shaul Mukamel as a research associate. He moved to Sungkyunkwan University in 2005, where he was promoted to professor in 2012. His research interest includes understanding molecular mechanisms of photocatalysts, electrocatalysts, batteries, organic light-emitting diodes (OLEDs), spin/electron transport, and excited-state dynamics based on computational approaches.

REFERENCES

(1) Asenbauer, J.; Eisenmann, T.; Kuenzel, M.; Kazzazi, A.; Chen, Z.; Bresser, D. The success story of graphite as a lithium-ion anode material-fundamentals, remaining challenges, and recent developments including silicon (oxide) composites. *Sustainable Energy Fuels* **2020**, *4* (11), 5387−5416.

(2) Li, R.; Lin, C.; Wang, N.; Luo, L.; Chen, Y.; Li, J.; Guo, Z. Advanced composites of complex Ti-based oxides as anode materials for lithium-ion batteries. *Adv. Compos. Hybrid Mater.* **2018**, *1* (3), 440−459.

(3) Abe, T.; Fukuda, H.; Iriyama, Y.; Ogumi, Z. Solvated Li-ion transfer at interface between graphite and electrolyte. *J. Electrochem. Soc.* **2004**, *151* (8), A1120.

(4) Nitta, N.; Wu, F.; Lee, J. T.; Yushin, G. Li-ion battery materials: Present and future. *Mater. Today* **2015**, *18* (5), 252−264.

(5) Manthiram, A. An outlook on lithium ion battery technology. *ACS Cent. Sci.* **2017**, *3* (10), 1063−1069.

(6) Meister, P.; Jia, H.; Li, J.; Kloepsch, R.; Winter, M.; Placke, T. Best practice: Performance and cost evaluation of lithium ion battery active materials with special emphasis on energy efficiency. *Chem. Mater.* **2016**, *28* (20), 7203−7217.

(7) Mao, C.; Wood, M.; David, L.; An, S. J.; Sheng, Y.; Du, Z.; Meyer, H. M.; Ruther, R. E.; Wood, D. L. Selecting the best graphite for long-life, high-energy Li-ion batteries. *J. Electrochem. Soc.* **2018**, *165* (9), A1837.

(8) Zhang, H.; Yang, Y.; Ren, D.; Wang, L.; He, X. Graphite as anode materials: Fundamental mechanism, recent progress and advances. *Energy Storage Mater.* **2021**, *36*, 147−170.

(9) Li, B.; Gao, X.; Li, J.; Yuan, C. Life cycle environmental impact of high-capacity lithium ion battery with silicon nanowires anode for electric vehicles. *Environ. Sci. Technol.* **2014**, *48* (5), 3047−3055.

(10) Chen, S.; Dai, F.; Cai, M. Opportunities and challenges of high-energy lithium metal batteries for electric vehicle applications. *ACS Energy Lett.* **2020**, *5* (10), 3140−3151.

(11) Wang, J.; Cheng, Y.; Zhu, Y.; Zhang, Q.; Zhang, H.; Zhao, C. Recent Progress on Performance Modulation and Mechanism Study of Silicon-Based Anodes. *Sustainable Energy Fuels* **2022**, *6*, 3094−3113.

(12) Kasavajjula, U.; Wang, C.; Appleby, A. J. Nano-and bulk-silicon-based insertion anodes for lithium-ion secondary cells. *J. Power Sources* **2007**, *163* (2), 1003−1039.

(13) Jin, Y.; Zhu, B.; Lu, Z.; Liu, N.; Zhu, J. Challenges and recent progress in the development of Si anodes for lithium-ion battery. *Adv. Energy Mater.* **2017**, *7* (23), 1700715.

(14) Su, X.; Wu, Q.; Li, J.; Xiao, X.; Lott, A.; Lu, W.; Sheldon, B. W.; Wu, J. Silicon-based nanomaterials for lithium-ion batteries: A review. *Adv. Energy Mater.* **2014**, *4* (1), 1300882.

(15) Chen, T.; Wu, J.; Zhang, Q.; Su, X. Recent advancement of SiO_x based anodes for lithium-ion batteries. *J. Power Sources* **2017**, *363*, 126−144.

(16) Hirata, A.; Kohara, S.; Asada, T.; Arao, M.; Yogi, C.; Imai, H.; Tan, Y.; Fujita, T.; Chen, M. Atomic-scale disproportionation in amorphous silicon monoxide. *Nat. Commun.* **2016**, *7*, 11591.

(17) Sun, Q.; Zhang, B.; Fu, Z.-W. Lithium electrochemistry of SiO_2 thin film electrode for lithium-ion batteries. *Appl. Surf. Sci.* **2008**, *254* (13), 3774−3779.

(18) Jung, S. C.; Kim, H.-J.; Kim, J.-H.; Han, Y.-K. Atomic-level understanding toward a high-capacity and high-power silicon oxide (SiO) material. *J. Phys. Chem. C* **2016**, *120* (2), 886−892.

(19) Yang, J.; Takeda, Y.; Imanishi, N.; Capiglia, C.; Xie, J.; Yamamoto, O. SiO_x-based anodes for secondary lithium batteries. *Solid State Ionics* **2002**, *152*−*153*, 125−129.
(20) Kim, H. J.; Choi, S.; Lee, S. J.; Seo, M. W.; Lee, J. G.; Deniz, E.; Lee, Y. J.; Kim, E. K.; Choi, J. W. Controlled prelithiation of silicon monoxide for high performance lithium-ion rechargeable full cells. *Nano Lett.* **2016**, *16* (1), 282−288.
(21) Zhao, J.; Lu, Z.; Liu, N.; Lee, H.-W.; McDowell, M. T.; Cui, Y. Dry-air-stable lithium silicide−lithium oxide core−shell nanoparticles as high-capacity prelithiation reagents. *Nat. Commun.* **2014**, *5*, 5088.
(22) Oumellal, Y.; Delpuech, N.; Mazouzi, D.; Dupre, N.; Gaubicher, J.; Moreau, P.; Soudan, P.; Lestriez, B.; Guyomard, D. The failure mechanism of nano-sized Si-based negative electrodes for lithium ion batteries. *J. Mater. Chem.* **2011**, *21* (17), 6201−6208.
(23) Xiao, H.; Fang, C.; Zheng, T.; Bai, H.; Liu, G. Investigation of SiO_x anode fading mechanism with limited capacity cycling. *APL Mater.* **2022**, *10* (1), 011108.
(24) Yuan, Q.; Zhao, F.; Zhao, Y.; Liang, Z.; Yan, D. Reason analysis for Graphite-Si/SiO_x/C composite anode cycle fading and cycle improvement with PI binder. *J. Solid State Electrochem.* **2014**, *18* (8), 2167−2174.
(25) Shi, L.; Wang, W.; Wang, A.; Yuan, K.; Jin, Z.; Yang, Y. Scalable synthesis of core−shell structured SiO_x/nitrogen-doped carbon composite as a high-performance anode material for lithium-ion batteries. *J. Power Sources* **2016**, *318*, 184−191.
(26) Hassoun, J.; Lee, K.-S.; Sun, Y.-K.; Scrosati, B. An advanced lithium ion battery based on high performance electrode materials. *J. Am. Chem. Soc.* **2011**, *133* (9), 3139−3143.
(27) Nam, D. H.; Hong, K. S.; Lim, S. J.; Kim, M. J.; Kwon, H. S. High-performance Sb/Sb_2O_3 anode materials using a polypyrrole nanowire network for Na-ion batteries. *Small* **2015**, *11* (24), 2885−2892.
(28) Kim, H.; Chou, C.-Y.; Ekerdt, J. G.; Hwang, G. S. Structure and properties of Li-Si alloys: A first-principles study. *J. Phys. Chem. C* **2011**, *115* (5), 2514−2521.
(29) Agubra, V. A.; Fergus, J. W. The formation and stability of the solid electrolyte interface on the graphite anode. *J. Power Sources* **2014**, *268*, 153−162.
(30) Rybaltovskiy, A. O.; Ischenko, A. A.; Zavorotny, Y. S.; Garshev, A. V.; Dorofeev, S. G.; Kononov, N. N.; Minaev, N. V.; Minaeva, S. A.; Sviridov, A. P.; Timashev, P. S.; Khodos, I. I.; Yusupov, V. I.; Lazov, M. A.; Panchenko, V. Y.; Bagratashvili, V. N. Synthesis of photoluminescent Si/SiO_x core/shell nanoparticles by thermal disproportionation of SiO: Structural and spectral characterization. *J. Mater. Sci.* **2015**, *50*, 2247−2256.
(31) Zhang, Y.; Guo, G.; Chen, C.; Jiao, Y.; Li, T.; Chen, X.; Yang, Y.; Yang, D.; Dong, A. An affordable manufacturing method to boost the initial Coulombic efficiency of disproportionated SiO lithium-ion battery anodes. *J. Power Sources* **2019**, *426*, 116−123.
(32) Li, J.; Guo, J.; Sun, Q.; Nie, X.; Dai, L.; Wang, Y.; Ci, L. Potassium Ions Regulated the Disproportionation of Silicon Monoxide Boosting Its Performance for Lithium-Ion Battery Anodes. *Energy Fuels* **2021**, *35* (19), 16202−16211.
(33) Xu, Q.; Sun, J. K.; Yin, Y. X.; Guo, Y. G. Facile synthesis of blocky SiO_x/C with graphite-like structure for high-performance lithium-ion battery anodes. *Adv. Funct. Mater.* **2018**, *28* (8), 1705235.
(34) Yang, X.; Zhan, C.; Xu, D.; Nan, D.; Lv, R.; Shen, W.; Kang, F.; Huang, Z.-H. SiO_x@Si-graphite microspheres for high-stable anode of lithium-ion batteries. *Electrochim. Acta* **2022**, *426*, 140795.
(35) Kwon, M.-J.; Maniyazagan, M.; Yang, H.-W.; Kang, W. S.; Kim, S.-J. A facile synthesis of vanadium-doped SiO_x composites for high-performance Li-ion battery anodes. *J. Alloys Compd.* **2020**, *842*, 155900.
(36) Yang, H.-W.; Lee, D. I.; Kang, N.; Yoo, J.-K.; Myung, S.-T.; Kim, J.; Kim, S.-J. Highly enhancement of the SiO_x nanocomposite through Ti-doping and carbon-coating for high-performance Li-ion battery. *J. Power Sources* **2018**, *400*, 613−620.
(37) Miyachi, M.; Yamamoto, H.; Kawai, H. Electrochemical properties and chemical structures of metal-doped SiO anodes for Li-ion rechargeable batteries. *J. Electrochem. Soc.* **2007**, *154* (4), A376.
(38) Tan, F.; Guo, H.; Wang, Z.; Niu, X.; Li, X.; Yan, G.; Wang, J.; Peng, W.; Hu, Q. Electrospinning-enabled SiO_x@TiO_2/C fibers as anode materials for lithium-ion batteries. *J. Alloys Compd.* **2021**, *888*, 161635.
(39) Liu, D.; Han, Z.; Yang, X.; Cheng, S.; Xie, J. Preparation of SiO_x@TiO_2@N-doped carbon composite using chitin as carbon precursor for high-performance lithium storage. *J. Alloys Compd.* **2022**, *891*, 162076.
(40) Xue, H.; Wu, Y.; Zou, Y.; Shen, Y.; Liu, G.; Li, Q.; Yin, D.; Wang, L.; Ming, J. Unraveling metal oxide role in exfoliating graphite: New strategy to construct high-performance graphene-modified SiO_x-based anode for lithium-ion batteries. *Adv. Funct. Mater.* **2020**, *30* (21), 1910657.
(41) Zhang, J.; Yang, G.; Wang, J.-A.; Hou, Z.-L.; Zhang, X.; Li, C. Graphene and carbon nanotube dual-decorated SiO_x composite anode material for lithium-ion batteries. *Energy Fuels* **2021**, *35* (23), 19784−19790.
(42) He, S.; Huang, S.; Wang, S.; Mizota, I.; Liu, X.; Hou, X. Considering critical factors of silicon/graphite anode materials for practical high-energy lithium-ion battery applications. *Energy Fuels* **2021**, *35* (2), 944−964.
(43) Tang, B.; He, S.; Deng, Y.; Shan, Y.; Qin, H.; Noor, H.; Hou, X. Advanced binder with ultralow-content for high performance silicon anode. *J. Power Sources* **2023**, *556*, 232237.
(44) Yan, J.; Zhao, X.; He, S.; Huang, S.; Qin, H.; Lou, H.; Hou, X. Artificial solid electrolyte interphase coating to reduce lithium trapping in silicon anode for highly stable lithium storage. *Surf. Interfaces* **2022**, *31*, 102029.
(45) Ren, Y.; Zhou, X.; Tang, J.; Ding, J.; Chen, S.; Zhang, J.; Hu, T.; Yang, X.-S.; Wang, X.; Yang, J. Boron-doped spherical hollow-porous silicon local lattice expansion toward a high-performance lithium-ion-battery anode. *Inorg. Chem.* **2019**, *58* (7), 4592−4599.
(46) Woo, J.; Baek, S.-H.; Park, J.-S.; Jeong, Y.-M.; Kim, J. H. Improved electrochemical performance of boron-doped SiO negative electrode materials in lithium-ion batteries. *J. Power Sources* **2015**, *299*, 25−31.
(47) Chen, Q.; Tan, L.; Wang, S.; Liu, B.; Peng, Q.; Luo, H.; Jiang, P.; Tang, H.; Sun, R. A facile synthesis of phosphorus doped Si/SiO_2/C with high coulombic efficiency and good stability as an anode material for lithium ion batteries. *Electrochim. Acta* **2021**, *385*, 138385.
(48) Jin, C.; Dan, J.; Zou, Y.; Xu, G.; Yue, Z.; Li, X.; Sun, F.; Zhou, L.; Wang, L. Carbon-coated nitrogen doped SiO_x anode material for high stability lithium ion batteries. *Ceram. Int.* **2021**, *47* (20), 29443−29450.
(49) Xie, W.; Pang, C.; He, P.; Xiao, C.; Koyama, M.; Wang, J.; Qi, X.; Ren, J.; He, X. Improving the performance of silicon monoxide anodes via tuning a multiple pre-doping system: A first-principles study. *Phys. Chem. Chem. Phys.* **2022**, *24* (12), 7405−7414.
(50) Chen, S.; Xu, Y.; Du, H. One-step synthesis of uniformly distributed SiO_x-C composites as stable anodes for lithium-ion batteries. *Dalton Trans.* **2022**, *51* (31), 11909−11915.
(51) Guo, X.; Xu, H.; Li, W.; Liu, Y.; Shi, Y.; Li, Q.; Pang, H. Embedding Atomically Dispersed Iron Sites in Nitrogen-Doped Carbon Frameworks-Wrapped Silicon Suboxide for Superior Lithium Storage. *Adv. Sci.* **2023**, *10*, 2206084.
(52) Wang, F.; Mao, J. Aerogel Constructed by Ultrasmall Mn-Doped Silica Nanoparticles for Superior Lithium-Ion Storage. *ACS Appl. Mater. Interfaces* **2021**, *13* (24), 28181−28187.
(53) Li, X.-D.; Zhao, Y.-M.; Tian, Y.-F.; Lu, Z.-Y.; Fan, M.; Zhang, X.-S.; Tian, H.; Xu, Q.; Li, H.-L.; Guo, Y.-G. Lithium/Boron Co-doped Micrometer SiO_x as Promising Anode Materials for High-Energy-Density Li-Ion Batteries. *ACS Appl. Mater. Interfaces* **2022**, *14* (24), 27854−27860.
(54) Liu, S.-F.; Kuo, C.-H.; Lin, C.-C.; Lin, H.-Y.; Lu, C.-Z.; Kang, J.-W.; Fey, G. T.-K.; Chen, H.-Y. Biowaste-derived Si@SiO_x/C

https://doi.org/10.1021/acs.energyfuels.3c00785
Energy Fuels XXXX, XXX, XXX−XXX

anodes for sustainable lithium-ion batteries. *Electrochim. Acta* **2022**, *403*, 139580.
(55) Han, J.; Jo, S.; Na, I.; Oh, S.-m.; Jeon, Y.-m.; Park, J.-g.; Koo, B.; Hyun, H.; Seo, S.; Lee, D.; Kim, H.; Kim, J.; Lim, J.-c.; Lim, J. Homogenizing Silicon Domains in SiO_x Anode during Cycling and Enhancing Battery Performance via Magnesium Doping. *ACS Appl. Mater. Interfaces* **2021**, *13* (44), 52202−52214.
(56) Tian, Y.-F.; Li, G.; Xu, D.-X.; Lu, Z.-Y.; Yan, M.-Y.; Wan, J.; Li, J.-Y.; Xu, Q.; Xin, S.; Wen, R.; Guo, Y.-G. Micrometer-Sized $SiMg_yO_x$ with Stable Internal Structure Evolution for High-Performance Li-Ion Battery Anodes. *Adv. Mater.* **2022**, *34* (15), 2200672.
(57) Liu, Z.; Yu, Q.; Zhao, Y.; He, R.; Xu, M.; Feng, S.; Li, S.; Zhou, L.; Mai, L. Silicon oxides: A promising family of anode materials for lithium-ion batteries. *Chem. Soc. Rev.* **2019**, *48* (1), 285−309.
(58) Huang, B.; Huang, T.; Wan, L.; Yu, A. Pre-lithiating SiO anodes for lithium-ion batteries by a simple, effective, and controllable strategy using stabilized lithium metal powder. *ACS Sustainable Chem. Eng.* **2021**, *9* (2), 648−657.
(59) Wan, W.; Zhang, Q.; Cui, Y.; Wang, E. First principles study of lithium insertion in bulk silicon. *J. Phys.: Condens. Matter* **2010**, *22* (41), 415501.
(60) Tabuchi, T.; Yasuda, H.; Yamachi, M. Li-doping process for Li_xSiO-negative active material synthesized by chemical method for lithium-ion cells. *J. Power Sources* **2005**, *146* (1−2), 507−509.
(61) Reynier, Y.; Vincens, C.; Leys, C.; Amestoy, B.; Mayousse, E.; Chavillon, B.; Blanc, L.; Gutel, E.; Porcher, W.; Hirose, T.; Matsui, C. Practical implementation of Li doped SiO in high energy density 21700 cell. *J. Power Sources* **2020**, *450*, 227699.
(62) Li, X.-D.; Zhao, Y.-M.; Tian, Y.-F.; Lu, Z.-Y.; Fan, M.; Zhang, X.-S.; Tian, H.; Xu, Q.; Li, H.-L.; Guo, Y.-G. Lithium/Boron Co-doped Micrometer SiO_x as Promising Anode Materials for High-Energy-Density Li-Ion Batteries. *ACS Appl. Mater. Interfaces* **2022**, *14* (24), 27854−27860.
(63) Li, G.; Li, J.-Y.; Yue, F.-S.; Xu, Q.; Zuo, T.-T.; Yin, Y.-X.; Guo, Y.-G. Reducing the volume deformation of high capacity SiO_x/G/C anode toward industrial application in high energy density lithium-ion batteries. *Nano Energy* **2019**, *60*, 485−492.
(64) Qi, C.; Li, S.; Yang, Z.; Xiao, Z.; Zhao, L.; Yang, F.; Ning, G.; Ma, X.; Wang, C.; Xu, J.; Gao, J. Suitable thickness of carbon coating layers for silicon anode. *Carbon* **2022**, *186*, 530−538.
(65) Guo, X.; Zhang, Y.-Z.; Zhang, F.; Li, Q.; Anjum, D. H.; Liang, H.; Liu, Y.; Liu, C.-s.; Alshareef, H. N.; Pang, H. A novel strategy for the synthesis of highly stable ternary SiO_x composites for Li-ion-battery anodes. *J. Mater. Chem. A* **2019**, *7* (26), 15969−15974.
(66) Ge, J.; Shen, H.; Zhou, F.; Li, Y.; Yuan, N.; Yang, W.; Zhou, H.; Xu, B.; Guo, R.; Xu, P. Oxygen-tailoring in SiO_x/C with a covalent interface for high-performance lithium storage. *J. Mater. Chem. A* **2022**, *10* (4), 1928−1939.
(67) Hu, Y. S.; Demir-Cakan, R.; Titirici, M. M.; Müller, J. O.; Schlögl, R.; Antonietti, M.; Maier, J. Superior storage performance of a Si@SiO_x/C nanocomposite as anode material for lithium-ion batteries. *Angew. Chem., Int. Ed.* **2008**, *47* (9), 1645−1649.
(68) Song, L.; Zhao, T.; Tan, X.; Mao, D.; Su, S.; Fan, Z.; Chu, W. Biomass-Derived Hierarchically Porous (Nitrogen, Phosphorus) Co-Doped SiO_x/C Composite Nanosheet Architectures for Superior Lithium Storage and Ultra-Long Cycle Performance. *Batteries Supercaps* **2022**, *5* (4), No. e202100350.
(69) Chen, W.; Xu, D.; Kuang, S.; Wu, Z.; Hu, H.; Zheng, M.; Yu, X. Hierarchically porous SiO_x/C and carbon materials from one biomass waste precursor toward high-performance lithium/sodium storage. *J. Power Sources* **2021**, *489*, 229459.
(70) Choi, I.; Lee, M. J.; Oh, S. M.; Kim, J. J. Fading mechanisms of carbon-coated and disproportionated Si/SiO_x negative electrode (Si/SiO_x/C) in Li-ion secondary batteries: Dynamics and component analysis by TEM. *Electrochim. Acta* **2012**, *85*, 369−376.
(71) Guo, J.; Zhai, W.; Sun, Q.; Ai, Q.; Li, J.; Cheng, J.; Dai, L.; Ci, L. Facilely tunable core−shell Si@SiO_x nanostructures prepared in aqueous solution for lithium ion battery anode. *Electrochim. Acta* **2020**, *342*, 136068.
(72) Wang, Z.; Yang, N.; Ren, L.; Wang, X.; Zhang, X. Core−shell structured SiO_x@C with controllable mesopores as anode materials for lithium-ion batteries. *Microporous Mesoporous Mater.* **2020**, *307*, 110480.
(73) Lv, P.; Zhao, H.; Gao, C.; Zhang, T.; Liu, X. Highly efficient and scalable synthesis of SiO_x/C composite with core−shell nanostructure as high-performance anode material for lithium ion batteries. *Electrochim. Acta* **2015**, *152*, 345−351.
(74) Liu, Z.; Zhao, Y.; He, R.; Luo, W.; Meng, J.; Yu, Q.; Zhao, D.; Zhou, L.; Mai, L. Yolk@Shell SiO_x/C microspheres with semi-graphitic carbon coating on the exterior and interior surfaces for durable lithium storage. *Energy Storage Mater.* **2019**, *19*, 299−305.
(75) Wang, H.; Que, X.; Liu, Y.; Wu, X.; Yuan, Q.; Lu, J.; Gan, W. Facile synthesis of yolk-shell structured SiO_x/C@Void@C nanospheres as anode for lithium-ion batteries. *J. Alloys Compd.* **2021**, *874*, 159913.
(76) Li, X.; Zhang, M.; Yuan, S.; Lu, C. Research progress of silicon/carbon anode materials for lithium-ion batteries: Structure design and synthesis method. *ChemElectroChem* **2020**, *7* (21), 4289−4302.
(77) Li, Z.; Yao, N.; Zhao, H.; Yang, Z.; Fu, B.; Wang, J. Communication—self-template fabrication of porous Si/SiO_x/C anode material for lithium-ion batteries. *J. Electrochem. Soc.* **2020**, *167* (2), 020555.
(78) Song, J.; Guo, S.; Kou, L.; Kajiyoshi, K.; Su, J.; Huang, W.; Li, Y.; Zheng, P. Controllable synthesis Honeycomb-like structure SiO_x/C composites as anode for high-performance lithium-ion batteries. *Vacuum* **2021**, *186*, 110044.
(79) Sun, L.; Su, T.; Xu, L.; Liu, M.; Du, H.-B. Two-dimensional ultra-thin SiO_x ($0 < x < 2$) nanosheets with long-term cycling stability as lithium ion battery anodes. *Chem. Commun.* **2016**, *52* (23), 4341−4344.
(80) Liu, N.; Lu, Z.; Zhao, J.; McDowell, M. T.; Lee, H.-W.; Zhao, W.; Cui, Y. A pomegranate-inspired nanoscale design for large-volume-change lithium battery anodes. *Nat. Nanotechnol.* **2014**, *9* (3), 187−192.
(81) Han, C.; Si, H.; Sang, S.; Liu, K.; Liu, H.; Wu, Q. Achieving fully reversible conversion in Si anode for lithium-ion batteries by design of pomegranate-like Si@C structure. *Electrochim. Acta* **2021**, *389*, 138736.
(82) Yu, Q.; Ge, P.; Liu, Z.; Xu, M.; Yang, W.; Zhou, L.; Zhao, D.; Mai, L. Ultrafine SiO_x/C nanospheres and their pomegranate-like assemblies for high-performance lithium storage. *J. Mater. Chem. A* **2018**, *6* (30), 14903−14909.
(83) Peng, H. J.; Huang, J. Q.; Cheng, X. B.; Zhang, Q. Review on high-loading and high-energy lithium-sulfur batteries. *Adv. Energy Mater.* **2017**, *7* (24), 1700260.
(84) Schulmeister, K.; Mader, W. TEM investigation on the structure of amorphous silicon monoxide. *J. Non-Cryst. Solids* **2003**, *320* (1−3), 143−150.
(85) Im, J.; Jang, E. K.; Kim, S.; Yoon, S.; Kim, D.-H.; Cho, K. Y. Two-dimensional, P-doped Si/SiO_x alternating veneer-like microparticles for high-capacity lithium-ion battery composite. *Chem. Eng. J.* **2020**, *402*, 126292.
(86) Yamamura, H.; Nobuhara, K.; Nakanishi, S.; Iba, H.; Okada, S. Investigation of the irreversible reaction mechanism and the reactive trigger on SiO anode material for lithium-ion battery. *J. Ceram. Soc. Jpn.* **2011**, *119* (1395), 855−860.
(87) Wang, Z.; Su, Q.; Deng, H.; He, W.; Lin, J.; Fu, Y. Q. Modelling and simulation of electron-rich effect on Li diffusion in group IVA elements (Si, Ge and Sn) for Li ion batteries. *J. Mater. Chem. A* **2014**, *2* (34), 13976−13982.
(88) Chou, C.-Y.; Hwang, G. S. Lithiation behavior of silicon-rich oxide ($SiO_{1/3}$): A first-principles study. *Chem. Mater.* **2013**, *25* (17), 3435−3440.
(89) Sivonxay, E.; Aykol, M.; Persson, K. A. The lithiation process and Li diffusion in amorphous SiO_2 and Si from first-principles. *Electrochim. Acta* **2020**, *331*, 135344.
(90) Liu, Q.; Ji, Y.; Yin, X.; Li, J.; Liu, Y.; Hu, X.; Wen, Z. Magnesiothermic reduction improved route to high-yield synthesis of

https://doi.org/10.1021/acs.energyfuels.3c00785
Energy Fuels XXXX, XXX, XXX−XXX

interconnected porous Si@C networks anode of lithium ions batteries. *Energy Storage Mater.* **2022**, *46*, 384−393.
(91) Zhu, B.; Liu, G.; Lv, G.; Mu, Y.; Zhao, Y.; Wang, Y.; Li, X.; Yao, P.; Deng, Y.; Cui, Y.; Zhu, J. Minimized lithium trapping by isovalent isomorphism for high initial Coulombic efficiency of silicon anodes. *Sci. Adv.* **2019**, *5* (11), No. eaax0651.
(92) Yu, Z.; Yu, K.; Wei, J.; Lu, Q.; Cheng, Y.; Pan, Z. Improving electrode properties by sputtering Ge on SiO anode surface. *Ceram. Int.* **2022**, *48* (18), 26784−26790.
(93) Van Duin, A. C.; Dasgupta, S.; Lorant, F.; Goddard, W. A. ReaxFF: A reactive force field for hydrocarbons. *J. Phys. Chem. A* **2001**, *105* (41), 9396−9409.
(94) Chenoweth, K.; Cheung, S.; Van Duin, A. C.; Goddard, W. A.; Kober, E. M. Simulations on the thermal decomposition of a poly(dimethylsiloxane) polymer using the ReaxFF reactive force field. *J. Am. Chem. Soc.* **2005**, *127* (19), 7192−7202.
(95) Senftle, T. P.; Hong, S.; Islam, M. M.; Kylasa, S. B.; Zheng, Y.; Shin, Y. K.; Junkermeier, C.; Engel-Herbert, R.; Janik, M. J.; Aktulga, H. M.; Verstraelen, T.; Grama, A.; van Duin, A. C. T. The ReaxFF reactive force-field: Development, applications and future directions. *npj Comput. Mater.* **2016**, *2*, 15011.
(96) Yang, H.; Huang, X.; Liang, W.; Van Duin, A. C.; Raju, M.; Zhang, S. Self-weakening in lithiated graphene electrodes. *Chem. Phys. Lett.* **2013**, *563*, 58−62.
(97) Huang, X.; Yang, H.; Liang, W.; Raju, M.; Terrones, M.; Crespi, V. H.; Van Duin, A. C.; Zhang, S. Lithiation induced corrosive fracture in defective carbon nanotubes. *Appl. Phys. Lett.* **2013**, *103* (15), 153901.
(98) Jung, H.; Yeo, B. C.; Lee, K.-R.; Han, S. S. Atomistics of the lithiation of oxidized silicon (SiO_x) nanowires in reactive molecular dynamics simulations. *Phys. Chem. Chem. Phys.* **2016**, *18* (47), 32078−32086.
(99) Ostadhossein, A.; Cubuk, E. D.; Tritsaris, G. A.; Kaxiras, E.; Zhang, S.; Van Duin, A. C. Stress effects on the initial lithiation of crystalline silicon nanowires: Reactive molecular dynamics simulations using ReaxFF. *Phys. Chem. Chem. Phys.* **2015**, *17* (5), 3832−3840.
(100) Ge, J.; Guo, T.; Shen, H.; Zhou, F.; Li, Y.; Yuan, N.; Yang, W.; Wang, Z.; Xu, Y.; Zhang, J.; Wu, Y. A. Regulating charge/ion transfer kinetic behavior via embedded TiO_x in hierarchical TiO_x/SiO_x@C with optimal expansion stress for lithium storage. *J. Power Sources* **2023**, *555*, 232357.
(101) Mai, W.; Yang, M.; Soghrati, S. A particle-resolved 3D finite element model to study the effect of cathode microstructure on the behavior of lithium ion batteries. *Electrochim. Acta* **2019**, *294*, 192−209.
(102) Wang, A.; Kadam, S.; Li, H.; Shi, S.; Qi, Y. Review on modeling of the anode solid electrolyte interphase (SEI) for lithium-ion batteries. *npj Comput. Mater.* **2018**, *4*, 15.
(103) Leung, K.; Soto, F.; Hankins, K.; Balbuena, P. B.; Harrison, K. L. Stability of solid electrolyte interphase components on lithium metal and reactive anode material surfaces. *J. Phys. Chem. C* **2016**, *120* (12), 6302−6313.
(104) Cheng, X. B.; Hou, T. Z.; Zhang, R.; Peng, H. J.; Zhao, C. Z.; Huang, J. Q.; Zhang, Q. Dendrite-free lithium deposition induced by uniformly distributed lithium ions for efficient lithium metal batteries. *Adv. Mater.* **2016**, *28* (15), 2888−2895.

https://doi.org/10.1021/acs.energyfuels.3c00785
Energy Fuels XXXX, XXX, XXX−XXX